HIF2α GENE DELETION IN SATELLITE CELLS RESCUES MUSCLE REGENERATIVE CAPACITY UNDER HYPOXIC CONDITIONS

by

YU-TSUNG MATTHEW WANG

(Under the Direction of Hang Yin)

ABSTRACT

Hypoxia, which is the condition where there is reduced oxygen concentration in the air, is a common condition in patients suffering from chronic obstructive pulmonary disease (COPD), peripheral artery diseases (PAD), and for people who live in high altitudes. Individuals under chronic hypoxic conditions suffer from muscle atrophy, a process where muscle homeostasis is disrupted and protein degradation occurs via the E3 ubiquitin proteasomal pathway. Under hypoxia, upregulation of hypoxia inducible factors (HIFs) control the stemness of muscle progenitor cells called satellite cells (SCs). We confirmed the delayed regeneration of tibialis anterior muscle in wildtype mice. Using a conditional gene deletion of Hif2α in Pax7+ SCs, we also observed rescue of muscle regenerative capacity in Hif2α KO mice under hypoxia at 13-14% O2. However, only a decrease in autophagic flux markers but not an increase in muscle atrophy markers in whole muscle could be confirmed.

INDEX WORDS: Hypoxia, Hif2α, muscle regeneration, autophagy, muscle atrophy.

HIF2α GENE DELETION IN SATELLITE CELLS RESCUES MUSCLE REGENERATIVE CAPACITY UNDER HYPOXIC CONDITIONS

by

YU-TSUNG MATTHEW WANG

B.S., University of Maryland – Baltimore County, 2013

A Thesis Submitted to the Graduate Faculty of The University of Georgia in Partial Fulfillment of the Requirements for the Degree

MASTER OF SCIENCE

ATHENS, GEORGIA

2017

HIF2α GENE DELETION IN SATELLITE CELLS RESCUES MUSCLE REGENERATIVE CAPACITY UNDER HYPOXIC CONDITIONS

by

YU-TSUNG MATTHEW WANG

Major Professor:	Hang Yin
Committee:	Jarrod Call
	Kevin K. McCully

Electronic Version Approved:

Suzanne Barbour
Dean of the Graduate School
The University of Georgia
May 2017

DEDICATION

I dedicate this thesis to my parents, for inspiring me to overcome my weaknesses and to stand back up.

ACKNOWLEDGEMENTS

I thank the University of Georgia for providing me this opportunity for advanced learning, and to my PI, Dr. Hang Yin, and lab members, Wenyan Fu, Yang Liu, Liwei Xie, Amelia Yin, whom have guided my experiments and helped me through this phase of my life. I also thank the committee members, Dr. Jarrod Call and Dr. Kevin McCully, for their support with the matter of my thesis project.

TABLE OF CONTENTS

Page

LIST OF TABLES

Page

LIST OF FIGURES

Page

CHAPTER 1

INTRODUCTION

Hypoxia is a condition where regions of tissues in the body are deprived of oxygen. Chronic hypoxic environments termed hypoxic environments are commonplace with individuals that live in high altitude locations, or suffer from pathological conditions such as chronic obstructive pulmonary disease (COPD) and peripheral arterial disease (PAD). Hypoxia can also impact a number of downstream biological functions such as angiogenesis, cell migration, cellular metabolism, and stem cell self-renewal (Gregg L. Semenza, 2016a). The plethora of different biological impacts suggest that multiple genetic and epigenetic pathways may be linked to these diseases. For patients who suffer from COPD and PAD, one comorbid symptom is muscle atrophy. Progressive muscle wasting is a complex problem that involves mechanisms such as oxidative stress, inflammatory cytokines, growth hormones and other enzyme regulations (Passey et al., 2016; Wüst & Degens, 2007). The amount of muscle atrophy is due to a combination of several factors, which includes hypoxia from airflow obstruction that leads to hypoxemia, malnutrition, disuse, and systemic inflammation (Wüst & Degens, 2007). Increased proteasomal degradation via the ubiquitin proteasome and decreased muscle synthesis are the results of these factors. Currently there are a number of treatments available to help COPD patients breathe better, which includes bronchodilators, various steroids to combat inflammation, and oxygen therapy. While oxygen therapy may help supplement the oxygen concentrations in the body, there is a

limit to the amount of oxygen that can be absorbed by the lungs in more severe cases of COPD due to diminished lung function. It is often thought that attenuating the muscle wasting portion of these associative symptoms may help delay the progression of the disease and improve patients' quality of life.

It is important to understand the mechanisms that allow for muscle wasting as it relates to muscle regeneration, since the mechanisms of muscle regeneration are similar to muscle homeostasis (Karalaki, Fili, Philippou, & Koutsilieris, 2009; Pallafacchina, Blaauw, & Schiaffino, 2013); They both rely on the satellite cell activation pathway to maintain or regenerate muscle cells. Currently, it is unclear exactly how hypoxia impacts the regenerative capacity from an acute injury, though current literature points towards a link between hypoxia and muscle atrophy. The focus of this study is to elucidate the role of a family of transcription factors called hypoxia-inducible factors (HIFs) and the role it plays in muscle regeneration and muscle atrophy.

Muscle maintenance and regeneration from an acute injury relies on a pool of muscle progenitor cells, known as satellite cells (SCs), that reside in a niche between the basal lamina and the sarcolemma of muscle cells (Mauro, 1961). Under normal circumstances, these satellite cells are mitotically quiescent and remain in this satellite cell niche until a stimulus causes them to activate (Karalaki et al., 2009). Upon muscle injury, these SCs leave the quiescent state and become mitotically active, where they begin to proliferate and differentiate to form mature myofibers after muscle damage. Muscle regeneration can be roughly divided into four phases **(Figure 1)**. Phase one is where necrosis of the damaged muscle cells take place and neutrophils and a heterogenous population of M1 and M2 macrophages infiltrate the injured muscle area

(Tidball, 2005). These cells provide a rich source of inflammatory cytokines and growth factors that are secreted into the muscle microenvironment, which serves to clean up the cellular debris left behind from the muscle injury and allows the muscle to make room for new growth. This usually takes place during the first couple days of muscle injury and may continue to manifest throughout muscle regenerative progression. Extension of this necrotic/proinflammatory phase has been shown to inhibit muscle regeneration, and also induces fibrosis due to increased extracellular matrix protein deposition in the muscle compartment (Mann et al., 2011).

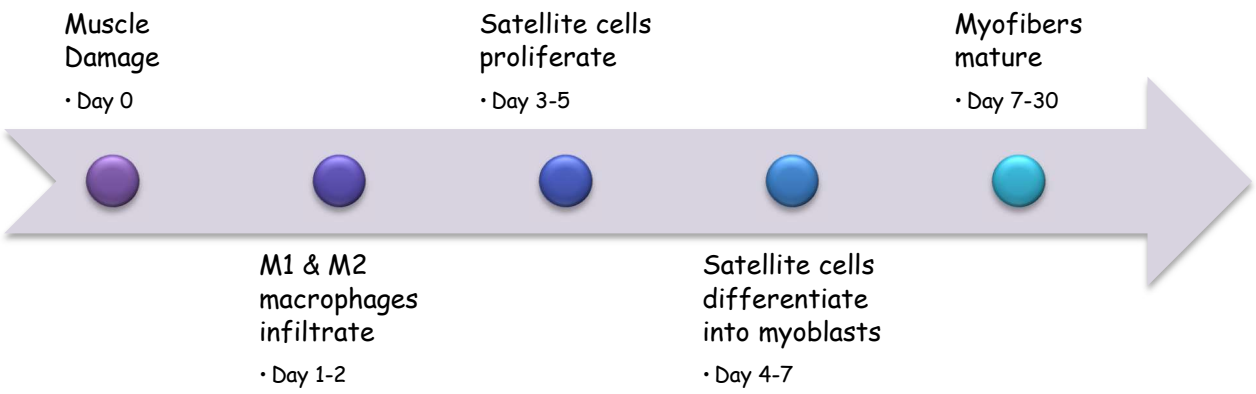

Figure 1 **Satellite cell myogenic progression during muscle regeneration.**

In phase two, SCs are activated from its quiescent state and re-enters the cell cycle through proliferation. Activated satellite cells normally express Pax7 during its quiescent state and expression decreases as the SC transitions from the proliferative phase to the differentiation stage. As the satellite cell proliferates, there are two myogenic cell fates that it can adopt once a SC successfully divides. The majority of proliferated satellite cells will continue on to differentiate into myoblasts, while a minor

population will self-renew and become quiescent satellite cells again (Kuang, Gillespie, & Rudnicki, 2008). This ability to self-renew is an important mechanism that allows muscle to retain its regenerative ability by replenishing its quiescent SC reserves for future muscle insults. Basic helix-loop-helix transcription factors known as myogenic regulatory factors (MRFs) are differentially expressed in these muscle regenerative phases in the determination of myogenic cell fate of SCs. These MRFs include Myf5, MyoD, myogenin (Myog), and MRF4. Depending on whether a SC self-renews or proceeds to differentiate, the SC can begin to upregulate MyoD as a deterministic factor that leads to differentiation, while the self-renewing SCs will simply express no MyoD, but still maintain Pax7 expression as it returns to the quiescent state (Karalaki et al., 2009).

In phase three of muscle regeneration, the committed myogenic satellite cells proceed to mature into myoblasts, where the nuclei migrate from the periphery and become centralized. Central nucleation is a telltale sign of newly regenerated muscle fibers. During this phase, MyoD and myogenin are expressed as indicators of differentiating myoblasts. By this point, Pax7 is no longer expressed. Finally, the myoblasts mature in phase four and they fuse with each other or with existing damaged myofibers to form multinucleated myofibers (Barberi et al., 2013; Karalaki et al., 2009). These various transcription factor regulations during each of these muscle regenerative phases can help pinpoint the state of muscle regeneration the muscle is currently in.

Specific Aim 1: To determine if delayed satellite cell myogenic progression can be rescued by Hif2α gene knockout under hypoxic conditions.

There is a class of proteins that are upregulated under hypoxia, known as hypoxia-inducible factors (HIFs). These HIFs are heterodimeric proteins that have an unstable α-subunit that is degraded under normoxic conditions, along with a constitutively stable ß subunit (Keith, Johnson, & Simon, 2011). Three isoforms of HIFs (HIF1α, HIF2α, HIF3α) have been discovered in mammals, where Hif1α and Hif2α proteins both contain conserved but different sets of two prolyl groups in what is known as the oxygen-dependent degradation domain (ODDD) (Dong et al., 2017). Under normoxic conditions, von Hippel-Lindau (VHL) tumor suppressors bind to the ODDD of the HIF α-subunit and the conserved prolyl groups are hydroxylated by prolyl hydroxylase domain proteins (PHDs), where it is later degraded via proteasomal degradation (Maxwell et al., 1999). Under hypoxia, VHL does not bind to HIFα subunits and results in HIF protein upregulation since they are not set up for proteasomal degradation.

Under hypoxic conditions, these HIFs have been implicated in several oncogenic pathways that can trigger cancerous characteristics such as angiogenesis, changes in metabolism, and metastatic nature of tumors (Krock, Skuli, & Simon, 2011; Liao, Corle, Seagroves, & Johnson, 2007; Liu, Semenza, & Zhang, 2015; G.L. Semenza, 2011). Studies have shown that once a tumor grows to become a certain size, it becomes more and more difficult for the tumor to receive the necessary blood flow within the core

of the tumor, thus creating a hypoxic environment in the innermost parts of the tumor (Gregg L. Semenza, 2016b). Many of the same oncogenic factors that promote tumor growth can be seen in muscle regeneration as well. For example, insulin-like growth factor binding protein 1 (IGFBP1) has been shown to be upregulated in cancerous tumors under hypoxic conditions, and these proteins have also been detected in regenerating muscle, suggesting that there may be a possible regulatory link via HIFs and muscle regeneration (Fu, Wang, & Hu, 2015; Tazuke et al., 1998).

Besides the possible common regulatory pathways that HIFs may impact on muscle regeneration, there have been studies that have shown how HIFs may be responsible for maintaining stemness, or also known as the ability for stem cells to self-renew and differentiate. One of the two major HIF subunits, HIF1α, has been shown to regulate cyclin dependent kinase inhibitors p21, p27, and p57, which keeps cell cycle progression in the G0 phase and prevents the cells from entering the G1 phase (Eliasson et al., 2010). HIF1α has also been shown to regulate pyruvate dependent kinases that are responsible for metabolism under anoxic conditions as a means for cellular adaptation to hypoxia (Kim, Tchernyshyov, Semenza, & Dang, 2006). HIF2α, the other majorly studied HIFα subunit, can be related to regulate key stemness transcription factors such as OCT4, SOX2, Nanog, Notch, and c-Myc (Boyer et al., 2005; Covello et al., 2006). These transcription factors have been linked to regulation of SC proliferation and differentiation. Of these transcription factors, OCT4 and Nanog overexpression in C2C12 myoblasts have been shown to prevent myotube formation and prevent terminal differentiation by suppressing MyoD expression (Lang et al., 2009). It is not surprising since OCT4 is one of the four transcription factors that is

upregulated to produce induced pluripotent stem cells from differentiated cell types (Takahashi & Yamanaka, 2006). A satellite cell is a quiescent stem cell that leans towards a myogenic cell fate, since it shares many of the same qualities as an adult stem cell. All these studies indicate that HIFs that are upregulated during hypoxic conditions may affect muscle regenerative capacity by altering the stemness of SCs.

Much of the research on HIFs was performed with the context of cancer biology in mind. As alluded to before, there are similarities in the way how cancer cells and satellite cells maintain their stemness and their entrance into the cell cycle, using similar transcription factors under hypoxic conditions. However, much of the research performed has mostly used an *in vitro* model or an *ex vivo* model with excised myofibers from experimental mice. If using the *in vitro* model to study HIFs, the C2C12 myoblasts were often placed under extreme hypoxic conditions such as 1-5% oxygen concentrations. For the purpose of mimicking whole-animal physiological responses under hypoxia, the aim of this study is to determine how muscle regenerative capacity is affected under hypoxic conditions using an *in vivo* mouse model, and whether HIF2α KO can attenuate any muscle regenerative defects associated with hypoxic conditions. In these experiments, mice under normoxia (room air) experienced the normal O2 concentration of 21%, while hypoxic mice were placed in chambers that were carefully monitored to maintain a steady oxygen concentration between 13-14% over the duration of the experiment. Normal saturated oxygen concentrated in arterial blood is 95%-98%, while anything above normal can be considered acceptable. With severe cases of COPD, these arterial saturated levels are reduced to below 90%.

Specific Aim 2: To understand whether autophagy plays a role in hypoxia-related muscle atrophy.

The other common observation is that hypoxic conditions can induce muscle atrophy, possibly due to less nutrition but more often primarily due to lower oxygen availability in the tissues overall. Muscle atrophy is driven by the ubiquitin-proteasome degradation pathway, which is regulated by a myriad of other factors such as atrogin-1 and MuRF-1. These genes are upregulated in response to stress signaling such as upregulation of reactive oxygen species from oxidative stress (Lőw et al., 2013), or induced inflammatory cytokines IL-10, TNF-α (Egerman & Glass, 2014; Yuan et al., 2015). These stress factors in turn lead to the ubiquitin-proteasomal degradation pathway that ultimately leads to the muscle atrophy phenotype.

Hypoxia has been shown to upregulate a multitude of enzymes and hormones that would collectively contribute towards the muscle atrophy phenotype. Leptin, which is a hormone that signals satiation, is upregulated under hypoxic conditions (Wang, Wood, & Trayhurn, 2008). Therefore, the upregulation of leptin should in theory reduce an animal subject's desire to feed. A transition of muscle fiber types from slow to fast has also been observed under hypoxia, which contributes to the fast-fatiguing symptoms in COPD patients (Gosker et al., 2002). As an essential component, lowered oxygen levels in muscle affect vital bodily processes such as glycosylation and ATP production within the mitochondria for life support. Some studies have proposed that increases in autophagic flux can contribute to muscle wasting (Sandri, 2010; Zhao et al.,

2007), so some of the groundwork has been laid out for the relationship between autophagy and muscle atrophy.

This aim focuses on the possibility that autophagy may play a role in determining muscle atrophy in a hypoxic environment. During the collection of preliminary data, it was noted that mice under severe oxygen tension from hypoxia lost weight very quickly during the first week. There are observations made during our preliminary study of mice in a hypoxic environment that demonstrates muscle atrophy over an extended period. The theory is, with lower oxygen consumption, the body has less oxygen available for oxidative phosphorylation. With less oxidative phosphorylation, less ATP is generated and consumed. The overall activity levels of the mice decrease. Less food intake means the body must go to other sources for its nutrients, which is a key trigger for autophagy. The body will first consume the adipose tissue that surrounds the essential organs then progress to skeletal muscle. At the cellular level, adipose cells and myogenic cells go through autophagy \to recycle to base materials necessary to produce ATP to keep bodily functions alive.

It has been shown that satellite cell progression into senescence is due to autophagy impairment in aged SCs (García-Prat et al., 2016). These satellite cells accumulate reactive oxygen species (ROS) that eventually leads to the cell's diminished ability to undergo proliferation. Autophagic flux is a measure of levels of autophagy. A part of sarcopenia, or age-related muscle wasting, is due to the SC's inability to retain the level of autophagic flux that is present in younger SCs. This type of autophagy mechanism may be triggered during chronic hypoxia; therefore, we hypothesize that inhibition of autophagy will positively affect muscle maintenance and reduce muscle

atrophy. We examined the tibialis anterior muscles of hypoxic mice to confirm the presence of autophagic markers LC3A/B and Atg12, as well as the muscle atrophy marker Atrogin-1, to correlate the relationship between autophagy and muscle atrophy.

CHAPTER 2

SCIENTIFIC APPROACH AND METHODS

To answer questions about hypoxia's impact on muscle regeneration in terms of satellite cells in a live mouse model, a suitable apparatus to induce hypoxia was necessary for these experiments. Other laboratories have explored the impact of hypoxia on satellite cells at a cellular level, where many *in vitro* studies have been employed to answer these specific questions (Chaillou & Lanner, 2016; Yang, Yang, Wang, & Kuang, 2017). However, those conditions that were conducted *in vitro* were often performed under extremely non-physiological conditions that involve pumping in excess carbon dioxide as the filler gas to produce hypoxic conditions. The hypoxic conditions created were often around 1-5% O2 for the acute hypoxia treatments. These *in vitro* studies can be considered proof-of-concept studies that demonstrate under how a satellite cell behaves under hypoxia. However, these studies do not completely mimic the SC microenvironment under hypoxia. Actual regeneration of muscle can only be performed in an *in vivo* animal model to better simulate the chronic hypoxic effect. Performing this type of experiment enabled us to look at both the phenotype and the underlying molecular mechanisms associated with muscle regeneration under these hypoxic conditions.

To answer the hypothesis proposed, we devised a series of hypoxia treatment experiments. The only way to collect meaningful data about hypoxia is to place the animal models under hypoxic treatment themselves. To do this, a series of 4 hypoxic

chambers were set up. These chambers were filled with a mix of proportional quantities of nitrogen gas and regular room air to achieve reduced oxygen levels within the chamber. This gas was constantly pumped into the chamber and excreted through an exit, where oxygen sensors detected the level of oxygen that exited the chambers. Experimental and control mice were placed into these chambers at very specific oxygen levels. There is a fine line between too little oxygen to maintain mouse survival, and not enough oxygen to induce a hypoxic effect on the mice. Therefore, we painstakingly experimented with different percentages of oxygen to achieve the best hypoxic conditions for these mice.

The most important aspect of this study was whether inhibiting Hif2α could rescue certain possible defects in cell proliferation or differentiation under the hypoxic environment. In the preliminary data, we have shown that a Hif2α KO mouse can retain more muscle mass under hypoxia compared to the wildtype control mice. In another piece of preliminary evidence, we showed that intramuscular (IM) injection of Hif2α inhibitor at the site of cardiotoxin injury can increase the amount of muscle regeneration. We hypothesized that inhibition of Hif2α may rescue the muscle regenerative defects under hypoxic conditions.

A few studies have performed *in vitro* work with SCs as it relates to muscle development and regeneration under hypoxic conditions (Chaillou & Lanner, 2016; Yang et al., 2017). In our proposed study, we aimed to expose experimental mice to normal atmospheric pressure, but with a reduced concentration of oxygen mixed into their air supply. This method is more feasible than hypobaric chambers to induce hypoxia because it is relatively inexpensive and only relies on accurate mixtures of

nitrogen gas and regular room air to attain the desired oxygen levels. To date, no other study has examined muscle regenerative capacity at an *in vivo* level under hypoxic conditions. Our preliminary studies indicated that 13%-14% oxygen levels were enough to induce a hypoxic effect and discern physiological differences, while keeping the mice alive long enough for the duration of the experiments.

A. Animal facility and treatment

All mice were housed in the Coverdell Rodent Vivarium (CRV) for the entirety of the experiment until tissue harvest. The animal rooms were placed under a 12-hour light and dark cycle. All experimental procedures were performed following the guidance of the University of Georgia Animal Use Proposal (A2014 02-002-Yi-A0) approved by the Institutional Animal Care and Use Committee (IACUC).

B. Mouse breeding and induction of conditional KO

Using Cre-LoxP technology, we developed a reliable conditionally inducible $Pax7^{CreER}$;$Hif2\alpha^{f/f}$ mouse model for these experiments. For our mouse model, tamoxifen induction of Cre recombinase at the Pax7 locus has been effective in knocking out any floxed gene targeted towards satellite cells . All mouse genotypes were confirmed with PCR. This was performed with solubilized ear clip samples from the mice before weaning at P14. Wildtype C57BL/6J mice were used in experiments as control. Knock out of the Hif2α gene from satellite cells was achieved by 2mg per 20g mouse body weight dosage of tamoxifen diluted in corn oil and delivered via intraperitoneal (IP) injections for three consecutive days to induce the conditional knockout. Control mice were given the same volume of corn oil via IP injections without tamoxifen, to eliminate

any result discrepancies due to differences in nutrition. To induce a genetic knockout, mice that contained Cre recombinase that has been fused with the ubiquitously expressed estrogen receptor (CreER) at the Pax7 satellite cell-specific locus was used to drive the Hif2α knockout gene expression in satellite cells (Gruber et al., 2007; Murphy, Lawson, Mathew, Hutcheson, & Kardon, 2011). 12-14-week-old (wko) $Pax7^{CreER}$;$Hif2\alpha^{f/f}$ mice at the start were used for these experiments, with a couple younger 7 wko exceptions in the 9 days post CTX experiment. For the conditional knock out of Hif2α to be satellite cell-specific, $Pax7^{CreER}$ mice were crossed with $Hif2\alpha^{f/f}$ to produce the experimental Hif2α KO mice. Since Hif2α deletion is embryonically lethal, a Cre-LoxP gene KO approach during the postnatal stage was utilized to perform these experiments. While tamoxifen was dissolved in corn oil for the Cre-LoxP knockout in the experimental mice, vehicle corn oil was injected into the control mice.

Upon IP injection of tamoxifen, CreER protein, that is localized in the cytoplasm of satellite cells, are translocated into the nucleus where the Hif2α transgene containing LoxP sites flanking Exon 2 (the DNA bHLH binding domain) is located (Gruber et al., 2007; Murphy et al., 2011). This produces a mutant mRNA transcript containing multiple in-frame stop codons downstream of exon 1 sequences, which stops translation of the gene (Gruber et al., 2007). Hence, only newly generated satellite cells from the proliferative cell cycle after SC activation can attain the Hif2α-less phenotype, and any existing Hif2α should be degraded via the oxygen-dependent proteasomal degradation pathway. In this study, only the homozygous $Pax7^{CreER}$; $Hif2\alpha^{f/f}$ mice were used for the experimental group. Some littermates that were heterozygous for floxed Hif2α were

used as a genetic control, as these mice were not given the tamoxifen injections to induce Cre recombinase translocation into the nucleus.

C. Hypoxia chambers

Our laboratory observed the phenomenon in wildtype mice that hypoxic mice tended to undergo muscle atrophy (data unpublished). There have been instances where attempts to perform intramuscular cardiotoxin injections on hypoxic mice proved to be very challenging because of the significant amount of muscle loss due to the hypoxic effect. In other words, sometimes when the hypoxic effect was too severe, there would be little muscle mass left for the mouse to regenerate from. This posed as an obstacle that had to be overcome. The idea was to generate optimal conditions for the hypoxia chambers to 1) Induce a hypoxic effect where a balance is struck between too much muscle atrophy and not enough muscle atrophy to be representative of the hypoxic effect, and 2) maintain mice survivability. Through a series of experiments, we arrived to the conclusion that the optimal hypoxic conditions that would induce enough muscle atrophy but still maintain enough muscle for us to examine are oxygen levels of between 13% and 14%. Normal oxygen levels at sea level elevation is 20.9%. The most direct method to monitor levels of hypoxemia in mice is to directly measure the O2 concentrations in blood via tail vein bleeds. However, we wanted to limit the amount of exposure of normal oxygen levels to the hypoxic mice to avoid reperfusion damage, therefore we used normal mouse behavioral observations such as hyperventilation and inactivity to gauge whether the mice experienced effects of hypoxia.

The hypoxia chamber setup was put together with instrumentation from Columbus Instruments. It contained several separate devices to make up the overall hypoxic chamber. A simplified outline of the hypoxia chamber instrument follows the series of steps below:

1. Regular room air and nitrogen gas (Airgas NI300) were each connected to a flow meter for air flow adjustments, and these parallel air lines were connected to a T fitting for mixing. These two flow meters were adjusted to create a mixing ratio that could achieve the target oxygen concentration. For example, if the target oxygen concentration is 15%, the air flow from the nitrogen tank would be increased on the nitrogen gas flow meter to increase the nitrogen to reference air ratio until the sensor readout was 15%. The outlet tube from the T-fitting contained the mixed gas that was transferred to the next step.
2. The mixed gas went through an ammonia filter to eliminate toxic ammonia buildup within the hypoxia chambers. The mixed gas also went through a series of desiccation tubes to eliminate moisture that could interfere with the oxygen and carbon dioxide sensor reading accuracy.
3. The filtered gas went through a sample pump, then went through an equalizer that evenly distributed the mixed gas into the connected hypoxia chambers. There was an inlet tube for the filtered mixed gas, and an outlet tube that sent the hypoxia chamber gas to the carbon dioxide and oxygen sensors for hypoxia chamber test readings. An overflow tube was located atop the chambers to prevent any excess pressure from building up within the chambers. Adequate bedding, food, and water were provided.

Both the carbon dioxide and oxygen sensors were calibrated each time a new nitrogen gas tank was connected. Ultra-high purity nitrogen gas (Airgas NI UHP 300) was used to calibrate the instrument to 0% oxygen levels. After the zero-point calibration, a specialized custom mixed gas canister with known concentrations of 20.50% O2 and 0.50% CO2, then balanced with N2 (Airgas X03NI79C3001005) was used to calibrate the instrument using the proper gain settings. This ensures that any unknown concentration of oxygen that passed through the hypoxia chamber would be read correctly by the sensors. The influx gas that went into the hypoxia chambers had a flow rate of 0.20L/min to 0.22L/min, which was sufficient to keep the air within the chamber at the desired concentration without hyposaturation of the mixed air. While oxygen concentration measurements could not be performed in real-time, the Oxymax program that was used to control the hypoxia instrument had functions that could test the oxygen concentration within the individual chambers over a user-designated period (set at 30s per reading). Multiple test readings in 10 minute intervals were taken to ensure that the oxygen levels could remain stable for the next 12 hours until the next oxygen concentration checkup. Mice were monitored at least twice a day to ensure accurate delivery of the proper concentration of mixed gas. These chambers were regularly rotated at random to ensure that there was no discrimination in air supply between the different chambers.

The mix of nitrogen and reference gas could only be maintained manually; There was no automatic gas injection system in place to monitor fluctuations in oxygen levels in the hypoxia chambers. We recorded oxygen concentration readings every 8-12 hours to maintain the appropriate oxygen levels within the chamber, since the nitrogen tank's

air pressure changes as it dispenses gas. Given that our hypoxia chamber apparatus has these limitations, we sought to maintain a constant ambient oxygen concentration within the chamber between a feasible range of 13% to 14%.

D. Tibialis anterior muscle injury by cardiotoxin treatment

Cardiotoxin (CTX) derived from snake venom is a potent myonecrotic substance that can cause complete acute muscle damage if administered properly. CTX injections were injected into the tibialis anterior (TA) and these muscles were harvested 4 days, 7 days, or 9 days later. Body weights were collected at the start of the hypoxic chamber treatment, during CTX injections that were usually combined with hypoxia chamber cleanings, and at the time of tissue harvest. One experimental mouse and one control mouse were paired up in the same chamber. Food and water were provided *ad libitum*, with minimum exposure to normal air if a food resupply was necessary. Chamber positions were cycled every day between mixed air input tubes to ensure that all chambers were supplied with equal amounts of mixed air. Normoxia control mice were kept in their original cages with full access to food and water. At the start of each hypoxia experiment, the mice were weighed before they were put into the hypoxia chambers that were pre-conditioned to 18% oxygen. For the following two days of initial hypoxia chamber setup, the oxygen were reduced by roughly 2% each day, until the target oxygen concentration reached the target 14%. Once the target oxygen concentration had been achieved, the mice were kept in the chambers for 7 days until intramuscular CTX injections in the left TA were given.

On the day of CTX injections, the body weights of mice were recorded. To maintain consistency in terms of damaging the muscle, the mice had to be briefly put under

anesthesia with isoflurane. The mice were given 5mg/kg body weight dosage of ketoprofen diluted in 0.9% saline solution as an analgesic prior to the CTX injections. 100μL of 5-10 μM CTX diluted in 0.9% saline solution were intramuscularly injected into the left TA muscles of both experimental and control groups with an insulin syringe that was coupled with a 28-gauge needle, while the contralateral TA remained uninjured. The mice were monitored carefully the following day after cardiotoxin injections for signs of distress and given an extra of ketoprofen if necessary.

At 4 days, 7 days, or 9 days after cardiotoxin injection (depending on the goal of the experiment), the mice were sacrificed and the injured left TA muscles and uninjured right TA muscles were harvested. The hypoxia chamber mice were kept in their chambers until time for sacrifice via cervical dislocation. Body weights were measured just prior to sacrifice. Injured and uninjured TA muscles were weighed, mounted vertically on 7% tragacanth gum with the distal end of the muscle pointing into the gum, and flash frozen in liquid nitrogen-cooled isopentane for a minute before transferred to a bucket of dry ice. These tissues were then stored in the -80C freezer or brought to the cryostat for immediate cryosectioning.

For cryosectioning, the TA muscles are transported from the -80C freezer to the -20C environment within the cryostat (Leica CM1850) and temperatures of the muscle tissues equilibrated for half an hour before cryosectioning began. 12 μm sections were collected and placed on a glass slide and dried for an hour before proceeding to the next experiment or stored in the -80C freezer for future analysis.

E. Immunostaining

Tissues were fixed with 2% paraformaldehyde and quenched with 50mM glycine. Incubation with primary antibodies for Pax7 (DSHB), Ki67 (Abcam), Laminin B2 (Millipore), eMyHC (DSHB), and myogenin (DSHB) were used for identifying muscle regenerative targets. Incubation with the appropriate secondary antibodies that are conjugated with AlexaFluor 488, AlexaFluor 546, and AlexaFluor 647 were used to visualize said markers under the fluorescent microscope. Hoechst 33342 was used as a nuclear counterstain that binds to the A/T-rich regions of dsDNA and does little to no staining of the cytoplasmic region. At one point in the experiment, we switched the muscle cell membrane stain from Laminin B2 to wheat germ agglutinin (WGA) for sarcolemma staining.

F. Analysis and statistical software

Tissue slides were visualized and pictures were captured on the fluorescent microscope. Using the Evos FL fluorescent microscope (Life Technologies), 5 to 7 representative images of damaged muscle areas were captured at 200x magnification to be representative of the muscle damage caused by CTX IM injection. All images were compared to a negative control background without the addition of any primary antibody. These images were quantitated and analyzed using ImageJ v1.51j software. Multiple cryosections from each TA sample were obtained and analyzed. All technical replicates of the tissues are representative of the damaged areas within the TA muscle compartment. Pax7+/Ki67+; Pax7+/Ki67- SCs were quantitated by examination of the 5-7 technical replicate images, where the Pax7 images had to be overlaid over the Ki67 images to observe colocalization of the fluorescent expression for these SCs. Myog+

cells were counted directly. CN number/ CN caliber: All centrally nucleated (CN) myofibers were overlaid with the laminin B2 (or WGA) images to get a clear outline of the newly regenerated myofibers. The regions of interest of these CN+ myofibers had to be manually selected using ImageJ software and quantitated in a Microsoft Excel spreadsheet, before finally migrating the data into Graphpad Prism 6.0. All relevant figures used a 2-sided unpaired t-tests performed at 95% CI for testing significance at $\alpha=0.05$ between the experimental group and the control group. Error bars shown in figures were based on the mean ± standard error of the mean (SEM).

G. Western blot analysis

Western blot analysis was performed against LC3-A/B (DSHB) and myosin heavy chain (DSHB). An 8% resolving gel was used. 30µg of tissue lysate were added to each well. SDS-PAGE gel ran at 80V for 1.5 hours. One hour of incubation in 5% nonfat dry milk diluted in tris-buffered saline with 0.1% Tween 20 (TBS-T) at room temperature. Protein transfer onto polyvinylidene difluoride (PVDF) membrane was performed overnight at 30V in 4C. PVDF After washes with TBS-T, PVDF membranes with primary antibody incubated in 4C overnight. Washes with TBS-T and one-hour room temperature incubation in secondary antibody is performed after the overnight primary antibody incubation. After secondary antibody incubation, the resulting PVDF membrane is exposed to a solution of Pierce ECL Western Blot Substrate (ThermoFisher. Cat. No. 32106). The membrane was then brought to the dark room for imaging onto autoradiography film (UltraCruz Autoradiography Film, Santa Cruz. Cat.

No. sc-201697). Afterwards, the amount of protein expression was normalized to the housekeeping protein myosin heavy chain as it is ubiquitous in muscle.

CHAPTER 3

RESULTS

Specific Aim 1: To determine if delayed satellite cell myogenic progression can be rescued by Hif2α gene knockout under hypoxic conditions.

Muscle regeneration is delayed in hypoxic mice versus normoxic mice

Muscle regeneration was examined in the two phases of muscle regeneration: the proliferative phase and the differentiation phase. Tissues were harvested from the experimental groups at specific timepoints after intramuscular cardiotoxin injection in the TA. Pax7 and Ki67 immunofluorescent expression were used to identify satellite cells and proliferating cells, respectively. Although Ki67 is a general biomarker for proliferating cells in all cell types, by examining the colocalization of Ki67 expression with satellite cells expression Pax7, we could identify those SCs that were proliferating at each time point. Ki67 expression also tapers once a cell has passed the proliferation stage, which effectively excludes any cells that have passed the proliferative phase and into the differentiation phase. Given this information, we excised four-day post cardiotoxin injury (dpi) TA muscle from mice that were under normoxia or hypoxia treatment, and performed fluorescent immunostaining against Pax7 and Ki67. Those that were classified as Pax7+/Ki67+ were deemed proliferating SCs, while the Pax7+/Ki67- cells were considered quiescent or self-renewing SCs. Given that Ki67 expression diminished after proliferation has ended, we could not tell the difference between those SCs that have never proliferated to those that have proliferated then

self-renewed to quiescence. An alternative stain such as injecting 5-ethynyl-2'-deoxyuridine (EdU), a thymidine analog used to directly measure de novo DNA synthesis, would have been useful to more permanently detect newly proliferated SCs that returned to quiescence, since the EdU incorporation becomes part of the DNA and does not degrade over time (Cavanagh, Walker, Norazit, & Meedeniya, 2011). However, failure to account for the time point in which EdU had to be injected to effectively quantify its uptake into the mouse's body during SC proliferation led to some inconsequential results with nonspecific cell type expression of EdU (data not shown). Even so, Ki67 expression was sufficient to identify those proliferative SCs during the proliferative phase of muscle regeneration.

The reduction in body weights in most mice during the experiment evaluated the impact of the hypoxia chamber on the physiology of the mice (Table 1). Between the initial body weights and the body weights recorded at the time of CTX injection, these mice have been exposed to a variable number of days of 14-15% oxygen hypoxia conditions. The data shows that body weights were not reduced for 5 out of 6 mice, which makes this level of hypoxia's effect on body weight inconclusive. However, 5 out of 6 mice had a reduction of body weight after the cardiotoxin injection. This may or may not translate into an effect via hypoxia during recovery from injury, but it shows that hypoxia combined with CTX injection negatively affected body weight. Further analysis of the histological data will confirm whether hypoxia affects muscle regeneration.

Table 1 **Body weights of mice under hypoxia/normoxia**

	Mouse #1 Hypoxia, 4dpi	**Mouse #2** Hypoxia, 4dpi	**Mouse #3** Hypoxia, 7dpi	**Mouse #4** Hypoxia, 7dpi	**Mouse #5** Normoxia, 4dpi	**Mouse #6** Normoxia, 7dpi
Initial body weight (BW)	21.86g	20.90g	21.74g	20.89g	19.16g	20.30g
BW at time of CTX injection	22.76g	22.03g	22.43g	22.55g	20.87g	20.00g
BW at TA harvest	20.30g	20.80g	21.60g	20.2g	19.50g	19.50g
BW difference	-1.56g	-0.10g	-0.14g	-0.69g	+0.34g	-0.80g

Immunofluorescent (IF) staining against embryonic myosin heavy chain (eMyHC) is an easy way to histologically discern the state of regeneration of a muscle. IF staining against eMyHC is shown in Figure 1 for the hypoxia- and normoxia-treated mice. In Figure 2A, the normoxic mouse showed robust eMyHC expression (red stain) in nearly all cells captured in this frame at 4 days dpi. Myoblast sizes were relatively uniform, although there were parts of the muscle compartment that showed ongoing necrosis. The same cannot be said of the hypoxic mice (Figure 2B); While eMyHC+ expression was rampant at 4 dpi, the shape of these eMyHC+ myoblasts had more atypical cell shapes. Under normal circumstances, 7 dpi is a point of muscle regeneration where eMyHC expression should be diminished with signs of central nucleation to indicate that the myoblast has entered the final stage of maturation. In Figure 2C, it shows that while there was still a lot of ongoing eMyHC expression, much of the muscle compartment had also completed differentiation and no longer expressed the embryonic form of

myosin heavy chain, shown in the darker areas. Those darker areas are centrally nucleated, which is indicative of progressive muscle regeneration past the eMyHC phase. It appears that the 7dpi time point hypoxic mouse (Figure 2D) showed similar eMyHC expression as the 4 dpi hypoxic mouse (Figure 2B), which indicates a slower regenerative response than the normoxic mouse. The histological data demonstrates two ideas: 1) 14-15% oxygen concentrations may be enough to induce a delay of muscle regeneration and, 2) the muscle regenerative profile is delayed under hypoxic conditions. Whether it is delayed during the proliferative or differentiative period can be further elucidated in the quantitative analysis of these cryosections.

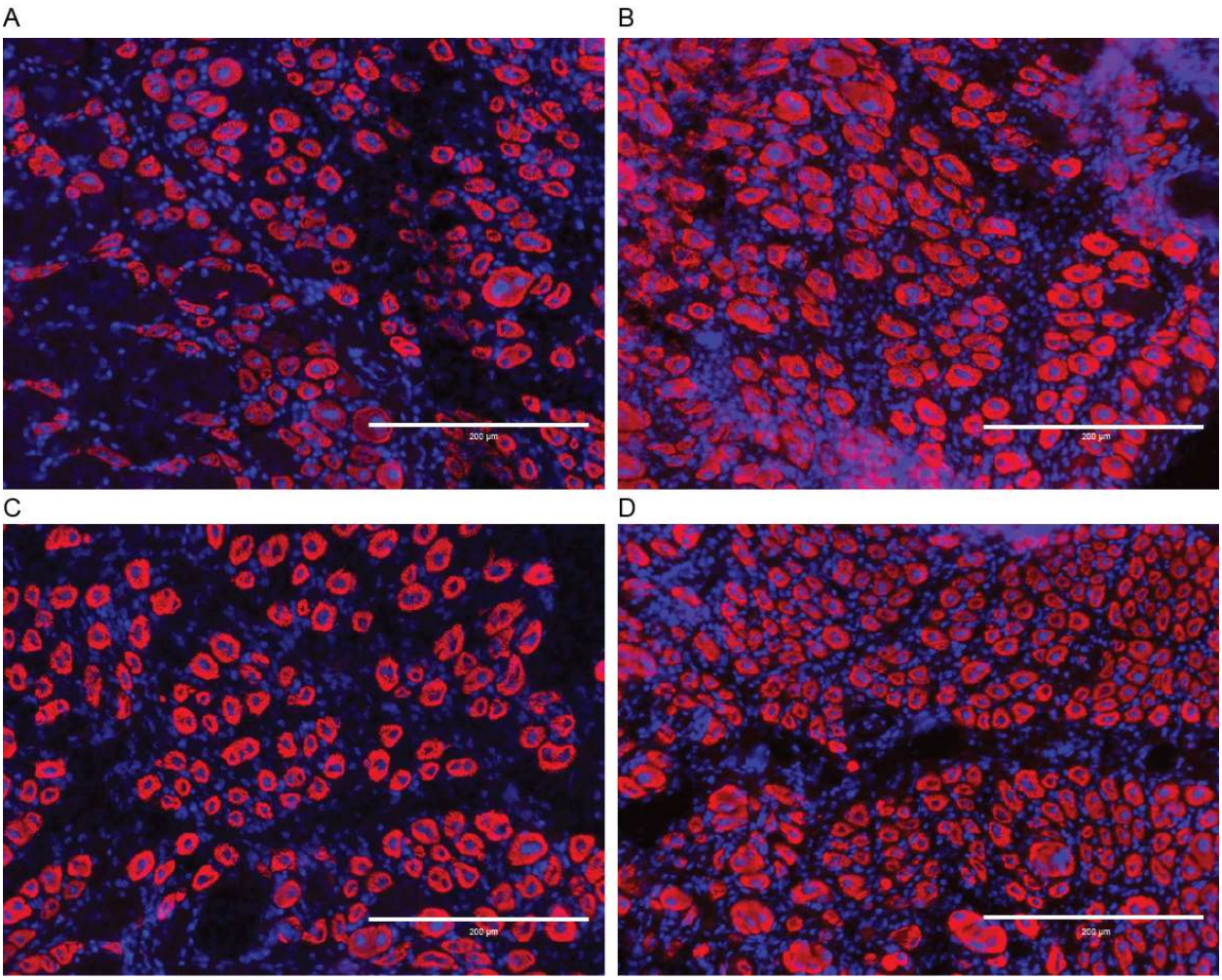

Figure 2 **Histological sections of hypoxic/normoxic muscle for wildtype mice.** Tibialis anterior (TA) muscles were excised at 4 days or 7 days post CTX. Fluorescent immunostaining against eMyHC (red) and DAPI (blue). Microscope pictures taken at 200x magnification. A: Normoxia. 4 dpi. B: Hypoxia. 4 dpi. C: Normoxia 7 dpi. D: Hypoxia. 7 dpi

Examining the specific transcription factors that are regulated, namely Pax7, Ki67, eMyHC, and myogenin, allows us to examine the state of regeneration at these different time points. Under normal circumstances, the proliferative stage should be at its peak at around 3-4 days post CTX injection, with signs of SC proliferation across the damaged portion of the muscle compartment. The 4-day post CTX time point shows that the number of proliferating SCs under hypoxic conditions were lower than normoxic mice, although not enough to achieve significance (Figure 3A, Appendix A). In terms of the amount of self-renewing SCs that were Pax7+/Ki67-, the reverse holds true where normoxic TA appears to have significantly more Pax7+/Ki67- SCs (Figure 3B). There are two possibilities why there were less proliferative SCs and more quiescent SCs. The first scenario is where normoxic mice are less progressed in muscle regeneration than the hypoxia mice, therefore there is a larger number of quiescent SCs that have not been activated yet. The other explanation would be that the normoxic mice have progressed further in muscle regeneration, where many of the proliferative cells have pushed towards differentiation and no longer express Ki67. From the histology figure in Figure 1, it is evident that the former is not the case, since there were many similarly-sized eMyHC+ myoblasts present at the 4 day dpi time point. It could be said that those increased number of quiescent Pax7+/Ki67- SCs have been renewed by this time point in the normoxia mice due to the number of proliferated SCs that have gone on to a myoblast cell fate. The proportional number of those proliferating SCs that returned to quiescence are shown in this example. Myogenin (Myog) expression was slightly higher in hypoxic mice (Figure 3C), while eMyHC+ myoblast sizes were bigger in hypoxic mice (Figure 3D). Given that only 2 mice were used for this 4 dpi group in this experiment, it

shows that the amount of regeneration can vary widely between littermates, where Mouse #1 lost a bigger proportion of its body weight after CTX treatment and Mouse #2 barely lost any weight, even though they resided in the same chamber. Despite these results, the overall state of the regenerating myofibers shown in Figure 1 clearly shows a trend where there is a rightward shift of the distribution curve of eMyHC+ cell sizes (Figure 3E); There were smaller sized eMyHC+ myoblasts in the hypoxic muscle than in the normoxic muscle. The high variability in the shapes and sizes shown in Figure 2A and 2B reflects this trend.

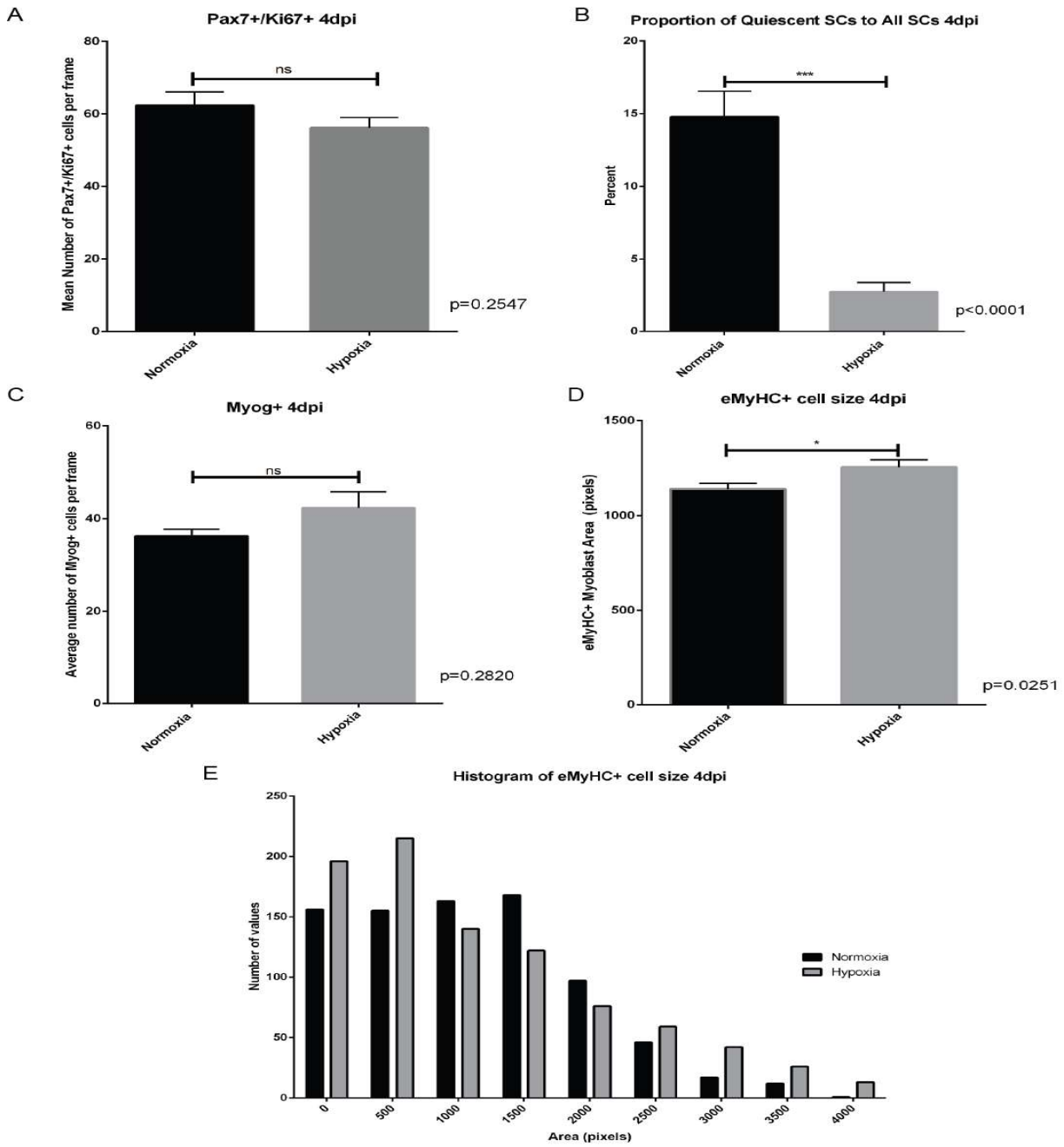

Figure 3 **Muscle regeneration at 4 dpi under normoxia/hypoxia for wildtype mice**. Quantitative analysis of TA muscle at 200x magnification. Hypoxia at 14%-15% oxygen concentration. Pax7 represents SCs, Ki67 represents proliferating cells, Myog represents differentiating cells, and eMyHC represents newly regenerated myofibers. 2-sided unpaired t-tests performed at 95% CI. Error bars are mean + s.e.m. Panel A, B, C: n number represents number of cryosections from 1 normoxia and 2 hypoxia mice. A: Number of proliferating SCs. n=3 (left), 7 (right). B: Number of quiescent SCs. n=3, 7. C: Number of differentiated myoblasts. n=4, 8. D: eMyHC+ myoblast sizes. n=821, 917. n is number of cells quantitated. E: Frequency distribution of all eMyHC+ myoblasts.

To further delve into whether muscle regeneration during the differentiation phase is different between normoxia and hypoxia, a 7 day post CTX time point was chosen. Usually by this time point under normoxia, those SCs that have proliferated will progress towards the differentiation phase to become myoblasts. eMyHC expression should be diminishing, with centralization of the nuclei to further indicate regeneration. In Figure 4A and 4B, they respectively show that the average number of Pax7+/Ki67+ and Pax7+/Ki67- SCs in the hypoxia group are reduced compared to normoxia. When comparing to the 4 dpi mice, the average number of proliferating SCs have also decreased significantly, which suggests that the proliferating SCs that were present at 4 dpi have progressed to the differentiated state (Appendix B). Since Myog+ and eMyHC+ expression is relatively consistent between normoxic and hypoxic groups (Figure 4C), this shows that the rates of proliferative SCs entering the differentiation state are similar. The number of proliferating SCs has been consistently high in the normoxia group, which means perhaps this mouse suffered from more CTX damage than the hypoxic mice. The other theory is that because this normoxic mouse was 4 weeks younger than the other mice (at the start of the experiment it was 7 weeks old), it was probably still undergoing a higher body growth rate than the other adult mice that had completed their growth phase. The most noticeable data gathered from these experiments are the increased centrally nucleated (CN) myoblast sizes in the normoxia mice. The hypoxia CN myoblasts were significantly smaller, and its distribution was shifted to the left when compared to normoxic myoblasts (Figure 4E, 4F). This means far fewer regenerating myoblasts have entered the final phases of regeneration. With these data, it confirms that there is delayed muscle regeneration under hypoxia.

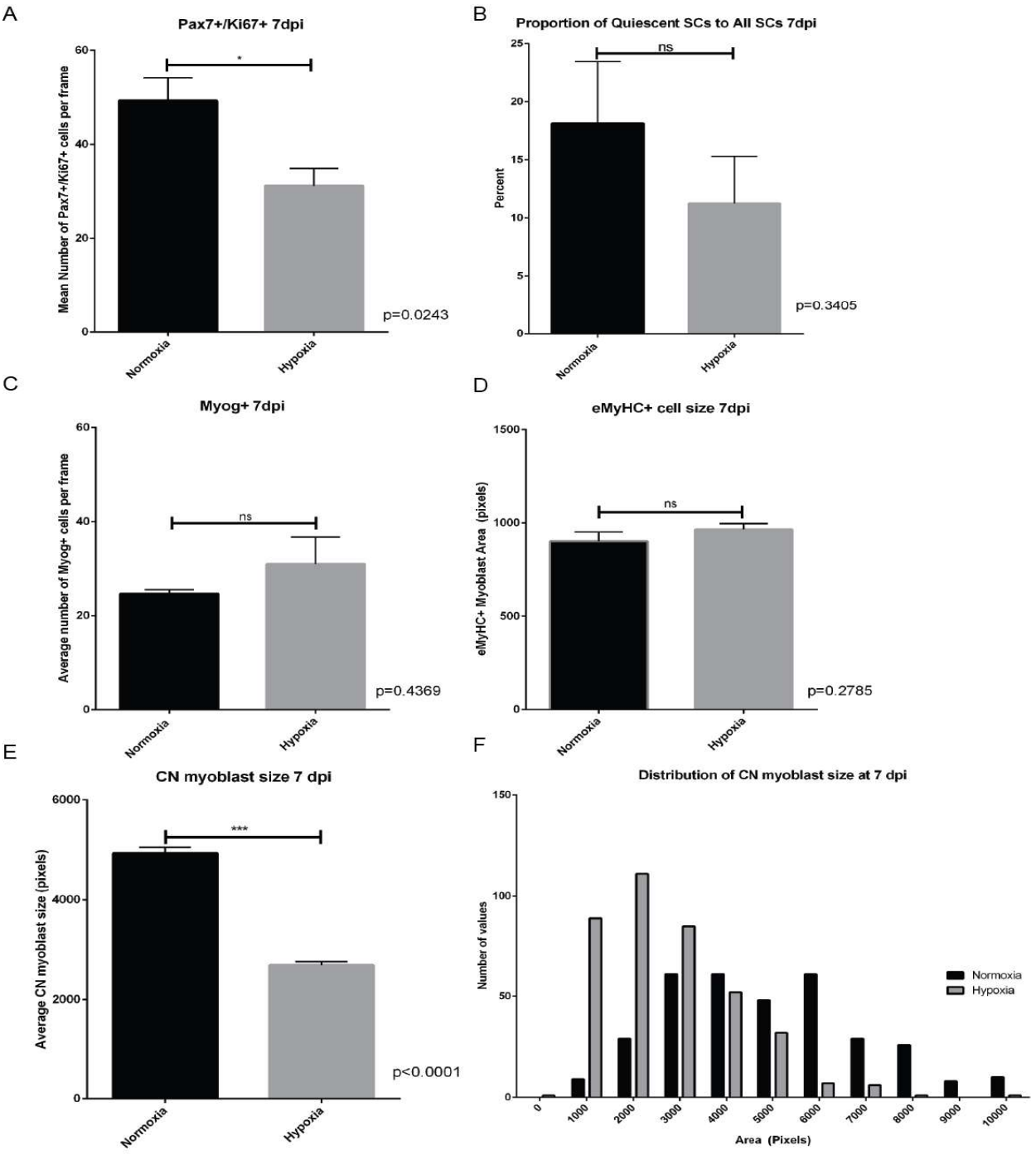

Figure 4 **Muscle regeneration at 7 dpi under normoxia/hypoxia for wildtype mice**. Quantitative analysis of TA muscle at 200x magnification. Hypoxia at 14%-15% oxygen concentration. 2-sided unpaired t-tests performed at 95% CI. Error bars are mean + s.e.m. Panel A, B, C: n number represent number of cryosections from 1 normoxia and 2 hypoxia mice. A: Number of proliferating SCs. n=3 (left), 5 (right). B: Number of quiescent SCs. n=3, 5. C: Number of differentiated myoblasts. n=3, 5. D: eMyHC+ myoblast sizes. n=498, 1312. n is number of cells quantitated. E: Frequency distribution of all eMyHC+ myoblasts.

Muscle regenerative capacity is rescued by Hif2α KO

Diminished muscle regenerative capacity has been confirmed in wildtype mice under hypoxic conditions, albeit with somewhat ambiguous results in terms of the normoxic mice. For the purposes of this study, the histological data suggests that there was a delay in the muscle regenerative response to injury. Given that hypoxia inducible factors are upregulated during hypoxia, we wanted to determine if knocking out these genes could affect the regenerative response in muscle. We chose Hif2α because there have been studies that have shown that it directly regulates the stemness of a stem cell, and it is also expressed in more chronic conditions of hypoxia. The other major HIF, Hif1α, is expressed during the initial exposure to acute hypoxia, and diminishes in expression after just a few hours in hypoxia as Hif2α expression takes over. As such, it made sense to use the Hif2α KO mouse model to study the differences in muscle regeneration over a relatively longer period of hypoxia exposure. These conditions are more representative of chronic pathological conditions experienced by COPD patients as well. Using Cre-recombinase technology to excise the Hif2α gene from satellite cells, along with our hypoxia instrument, we examined the *in vivo* muscle regenerative response under hypoxia.

Two time points were set for these experiments, where the same 4 dpi for proliferation was chosen, but a 9 dpi time point was used instead of 7 dpi to show a bigger difference between the amount of regeneration and to demonstrate any major differences in the rate of differentiation. Given that the mouse body weights of the normoxia versus hypoxia experiment were not significantly affected, oxygen concentrations were reduced by an additional 1%, down to 13%-14%, for a presumably

more robust hypoxic effect while maintaining mouse survivability. At the 4 dpi time point, the number of proliferating SCs in the Hif2α KO mouse was significantly lower than that of the control mouse (Figure 5A, Appendix C). The number of quiescent SCs were also significantly lower at this time point (Figure 5B). The lower amount of identifiable Pax7 SCs in both quiescent and proliferating states may indicate more have transitioned to a Pax7- differentiating/differentiated state. This is supported by the average number of myogenin+ myoblasts were slightly higher in the KO (Figure 5C), and eMyHC cell sizes were significantly higher as well (Figure 5D). It is also apparent that under the microscope, nearly 100% of the regenerating myofibers are strongly expressing eMyHC in both control and knockout mice at 4 dpi. A rightward shift in the distribution curve for sizes of eMyHC+ myoblasts is similar to the trend observed in Figure 3E with normoxic mice injury recovery (Figure 5E). This suggests that the knockout mouse exhibited signs of regeneration at the proliferative phase that was comparable to regeneration in normoxia. Between the increased myogenin expression and larger eMyHC+ myoblasts, this may be indicative of a more progressive regenerative response early in the time course of regeneration in the Hif2α knockout. Moreover, accounting for the lower average number of proliferating SCs, it suggests that those SCs in the KO mouse have already proliferated and moved on to the differentiation phase.

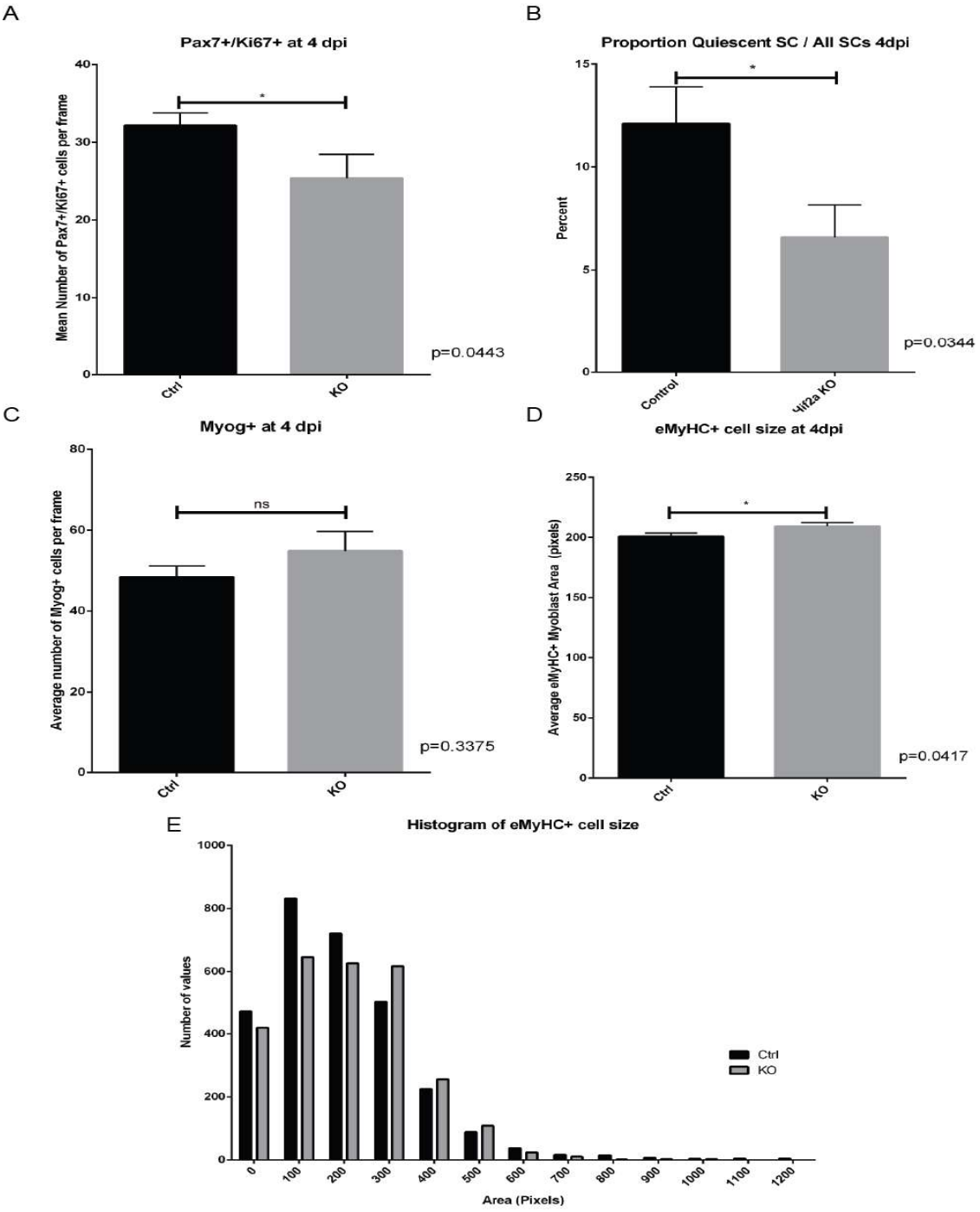

Figure 5 **Muscle regeneration at 4 dpi under hypoxia for Hif2α KO mice.** Quantitative analysis of TA muscle at 200x magnification. Hypoxia at 13%-14% oxygen concentration. 2-sided unpaired t-tests performed at 95% CI. Error bars are mean + s.e.m. Pane A, B, C: n number represents number of cryosections from 1 control and 1 hypoxia mouse. A: Number of proliferating SCs. n=18 (left), 13 (right). B: Number of quiescent SCs. n=18, 13. C: Number of differentiated myoblasts. n=8, 13. D: eMyHC+ myoblast sizes. n=2929, 2713. n is number of cells quantitated. E: Frequency distribution of all eMyHC+ myoblasts.

The 9 dpi time point was examined for any differences in the differentiation phase of muscle regeneration. The eMyHC expression in these sets of mice evaluated the variability in muscle regeneration between the two groups. The control mouse still retained a lot of necrotic debris in the darker regions of the frame, and eMyHC+ cells were not similar in shape and size (Figure 6A). The eMyHC expression was slightly diminished compared to the 4 dpi image, but it was nowhere near the level of faded expression shown in the Hif2α KO (Figure 6B). The histology of this mouse shows that much of the eMyHC expression have matured into more adult forms of myosin heavy chain and those that are in the darker areas but still showed central nucleation were those myoblasts near regeneration completion. When quantitating these images for Pax7, Ki67, eMyHC, and Myog immunostaining, the levels of expression have similar or more contrast to the 4 dpi time point. The average number of proliferating SCs was still significantly lower in the KO mouse, but both groups showed a dramatic increase in the number of quiescent SCs compared to 4 dpi, with the KO having slightly higher numbers than the control (Figure 6C, 6D, Appendix D). Myogenin, which had thus far not been able to demonstrate any significant differences and only slight changes in expression in previous experiments, finally showed a significantly lower amount of expression in the Hif2α KO (Figure 6E). Similarly, the number of eMyHC+ cells in the KO was significantly lower (Figure 6F), although the overall sizes of these cells were not different. At this time point, it was also possible to stain against the extracellular matrix proteoglycans with WGA, so cell sizes of centrally nucleated myoblasts were manually quantitated. Figure 6G shows that those new regenerated myofibers in the KO have myoblasts that were significantly bigger than the control. The overall distribution curve

of the myofiber caliber have also shifted right towards more myoblasts being larger than control (Figure 6H).

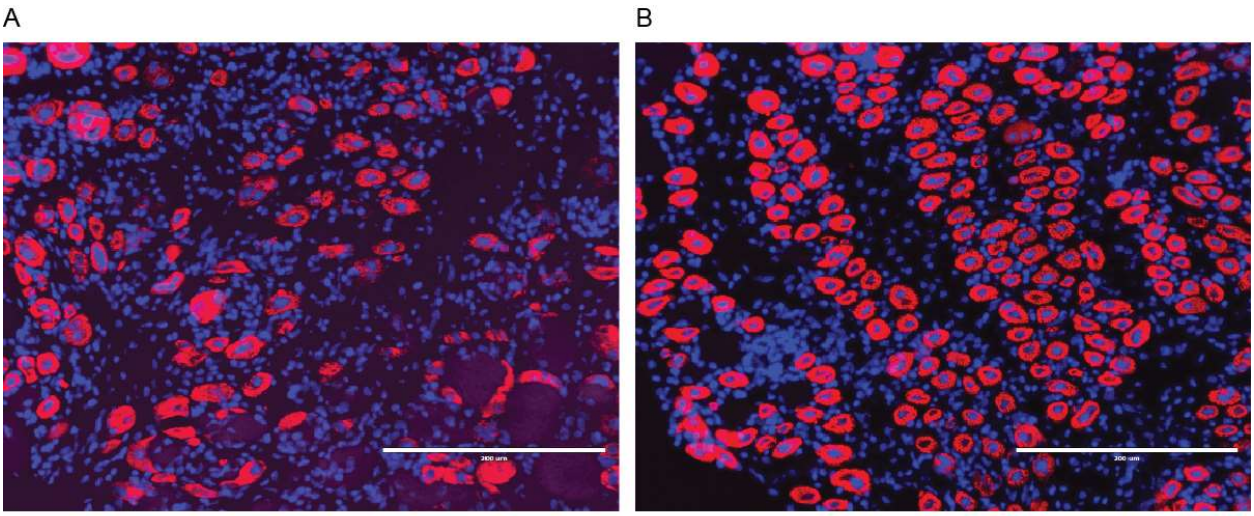

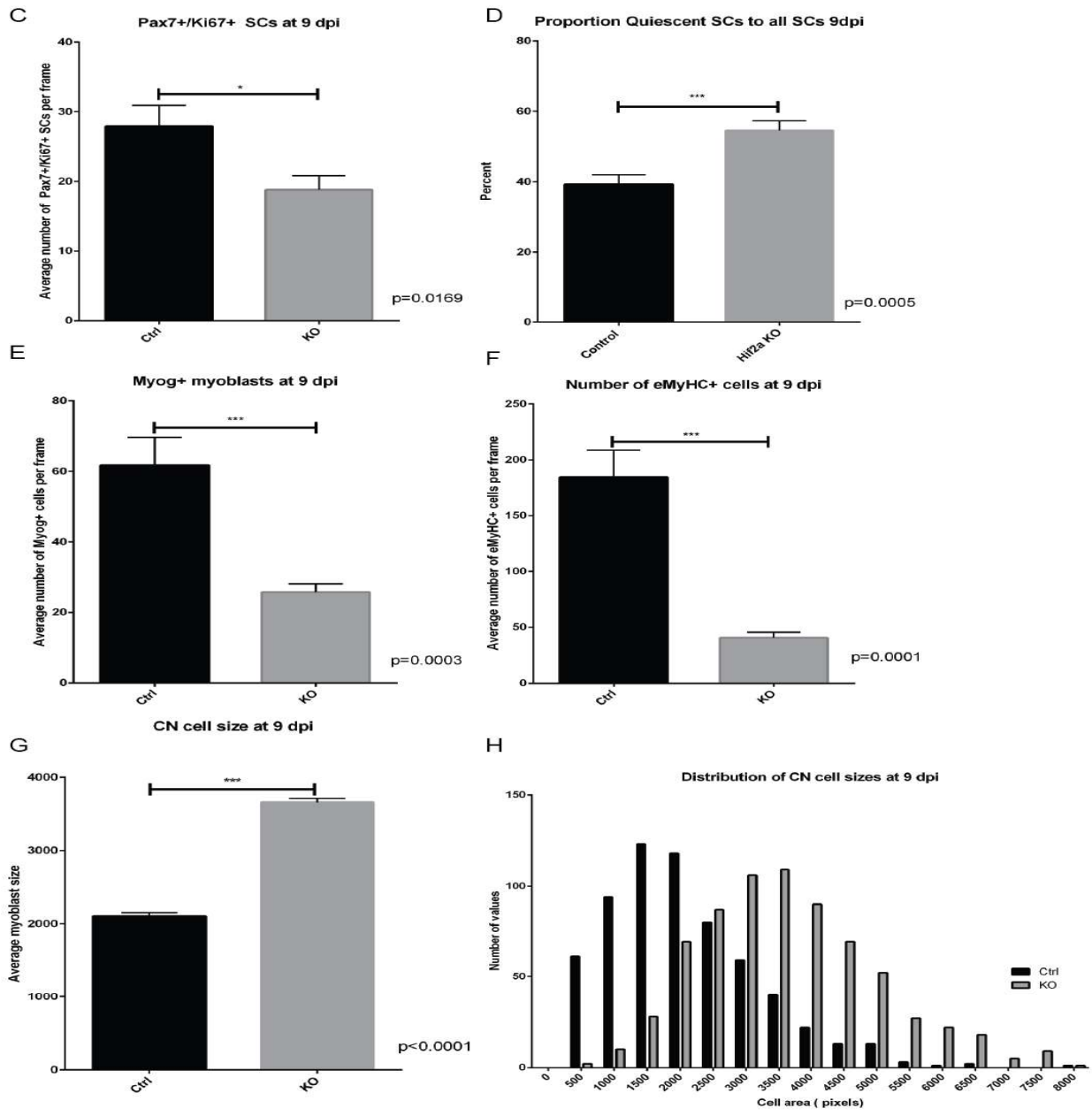

Figure 6 **Muscle regeneration at 9 dpi under hypoxia for Hif2α KO mice.** Quantitative analysis of TA muscle at 200x magnification. Hypoxia at 13%-14% oxygen concentration. 2-sided unpaired t-tests performed at 95% CI. Error bars are mean + s.e.m. Panel C, D, E: n number represents number of cryosections from 2 control and 2 hypoxia mice. A: IF eMyHC expression (red) control. B: IF eMyHC expression (red) Hif2α KO. C: Number of proliferating SCs. n= 16 (left), 16 (right). D: Number of quiescent SCs. n=16, 16. E: Number of differentiated myoblasts. n=9, 10. F: eMyHC+ myoblast sizes. n=2852, 556. n is number of cells quantitated. G: CN cell size. n= 630, 708. n is number of cells quantitated. H: Frequency distribution of all eMyHC+ myoblasts.

Possible adaptation to the hypoxic environment

Finally, changes in mouse body weights over the duration of the experiments were plotted. Body weight is a quick way to identify signs of muscle atrophy and changes in muscle homeostasis, where weight loss allows us to quickly ascertain a loss of muscle mass due to a hypoxia. Changes in body weight were recorded over the course of the 4 dpi and 9 dpi hypoxia experiments for signs of muscle atrophy. In Figure 7, Group 1 (4 dpi) and Group 2 (9 dpi) both suffered from weight loss up until the day of cardiotoxin injection after 9 days in the hypoxic chamber. Group 3 somehow increased its body weights during the experimental period. An explanation for this may be that these mice were still not fully grown adult mice (7 weeks old) at the start of the hypoxic chamber experiment. The age of such mice probably still had plenty of room for growth during the three-week experiment, which may have skewed their body weight results, whereas the rest of the mice were 11 weeks old at the beginning of their respective experiments. Interestingly, the body weights of Group 1 and Group 2 increased steadily after cardiotoxin injury, even though most never fully recovered their initial body weights by the end of the experiment. These body weights may be an indication of some form of adaptation to the hypoxic environment. During the first week of the hypoxia experiment, the mice of these two groups suffer from loss of body weight. Afterwards from the CTX injection time point until the end of the experiment, however, both control and Hif2α KO mice have an increase in body weight. This may point to a form of adaptation to their hypoxic environment after prolonged exposure to the same level of hypoxia.

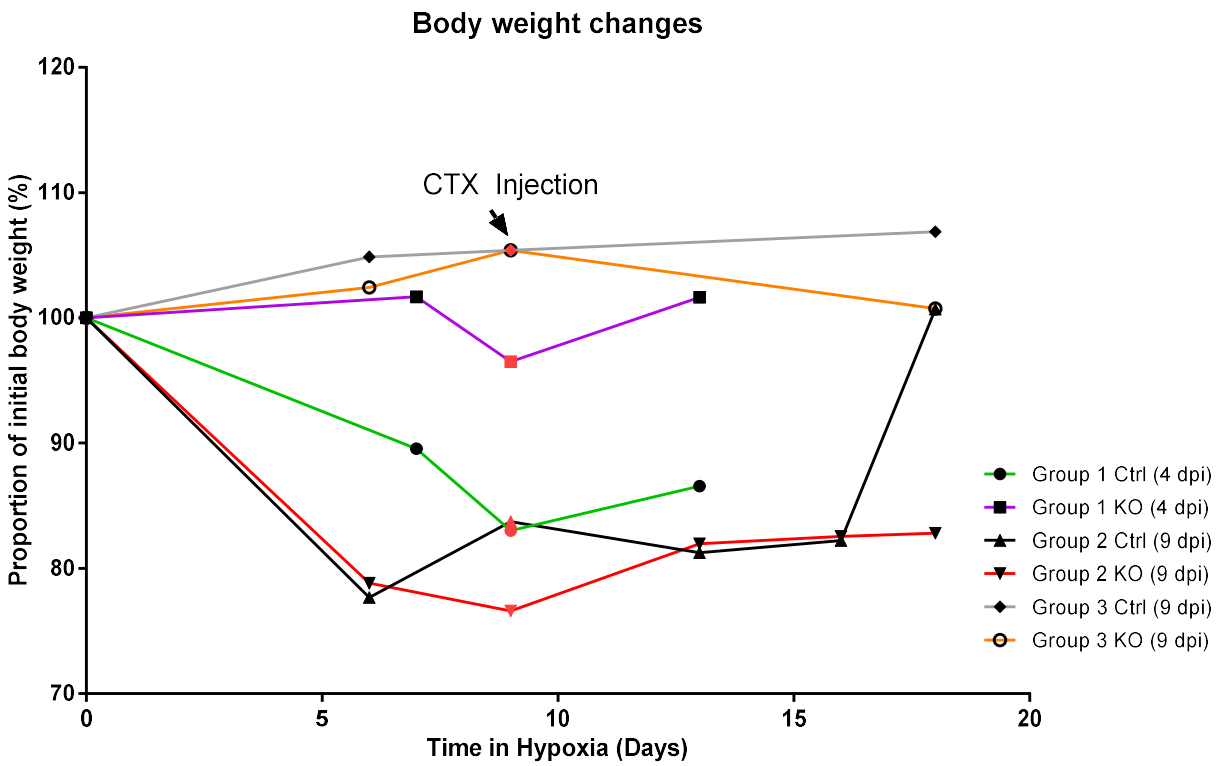

Figure 7 **Body weight changes over the experiment.** Body weights of 4 dpi and 9 dpi mice were recorded at different time points. The red markers indicate the date of cardiotoxin injection into the TA muscle after 9 days in hypoxia.

Specific Aim 2: To understand whether autophagy plays a role in hypoxia-related muscle atrophy.

In this specific aim, we wanted to correlate muscle atrophy with autophagic dysregulation in whole muscle. Muscle lysates from uninjured TA muscles of normoxic and hypoxic mice were used for Western blot analysis against common autophagy biomarkers such as Atg12 and LC3A/B. Of all the body weights recorded, Hypoxia Mouse 1 lost the most body weight, since it was retained in a hypoxic environment for a longer length of time than the rest of the mice (Figure 8A). With Western blot analysis, Atg12 is faintly expressed in normoxic uninjured TA, and even less so in hypoxic uninjured TA (Figure 8B). However, LC3A/B is reduced in the Hypoxia Mouse 2 lane, whereas both normoxia mouse lanes express much higher levels of LC3A/B. In Hypoxia Mouse 1, given that probably more protein was loaded into that lane due to the thicker band of MHC control, it generated the proportional amount of LC3A isoform, but the LC3B isoform remained much lower than the normoxic mice. These results indicate that autophagy is inhibited in the hypoxic mouse, given that the expression of Atg12 and LC3B are both lower in the hypoxic mice than the normoxic mice. The muscle atrophy marker, Atrogin-1, was also a target in this Western Blot analysis. Unfortunately, the analysis yielded no Atrogin-1 expression. Multiple repetitions of the Western blotting analysis were performed to get a protein band, but the conclusion is that there was no Atrogin-1 present in these lysate samples. One possibility for this phenomenon could be that these mice were not undergoing constant protein degradation at that level of

oxygen deprivation, but it was enough to induce an effect in terms of muscle regenerative capacity. When examining some of the injured and uninjured TA muscles from past experiments, it is not obvious that the hypoxic uninjured TA were much different than normoxic uninjured TA without closer examination of the cryosections (Figure 8C). When tallying the percent body weights of the uninjured TA muscles across multiple hypoxic chamber experiments at 13-15% oxygen, it yielded an average percentage body weight that was lower than that of normoxic TA muscle, but remained statistically insignificant (Figure 8D). Hence, the hypothesis that autophagy may regulate muscle atrophy is unconfirmed.

A

	Normoxia 1	Normoxia 2	Hypoxia 1	Hypoxia 2
Initial body weight at time for CTX injection	19.7g	20.54g	27.19g	22.62g
Final body weight at time of CTX injection	19.2g	19.3g	21.3g	22.2g

C

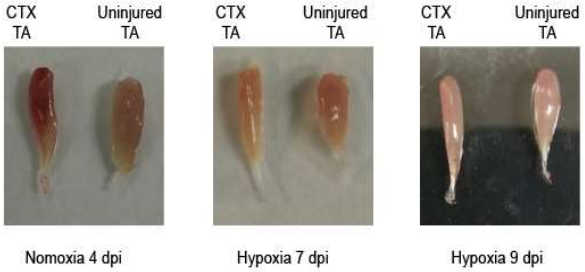

B

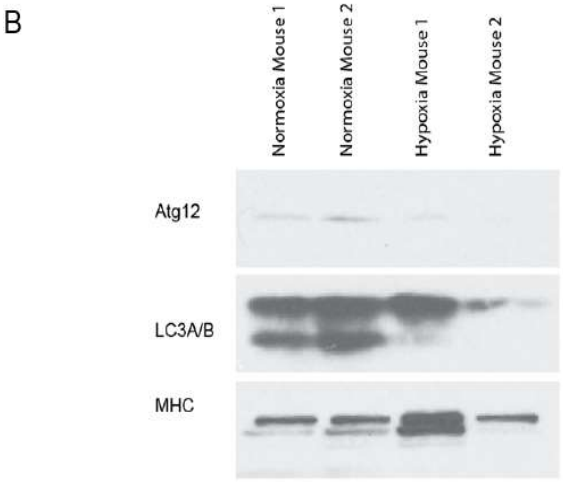

D

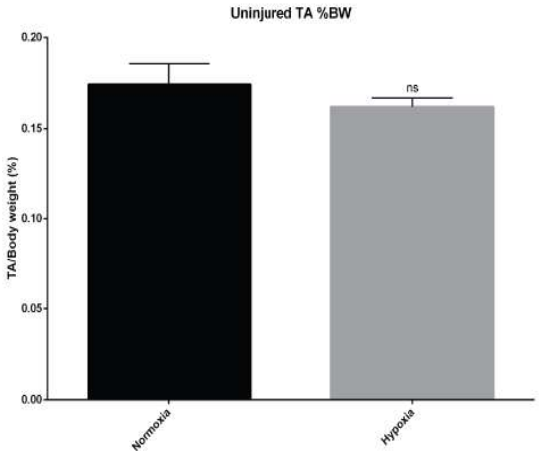

Figure 8 **Western blot analysis with normoxic and hypoxic mice in uninjured TA.** A. Changes in body weight as an indicator for muscle atrophy. Muscle lysates were obtained and normalized for further Western blot analysis. B. Western blot analysis. 30µg protein sample loaded per lane. Atg12 and LC3A/B are autophagy biomarkers. Myosin heavy chain (MHC) is the loading control. C. TA muscle pictures at time of muscle harvest. No visible difference between normoxia and hypoxia muscles. D. 2-sided unpaired t-test performed at 95% CI. Error bars are mean + s.e.m. Percent body weight of uninjured TA muscle across all experimental mice under normoxia and hypoxia environment. Slight reduction in TA weight but statistically insignificant. Normoxia n=3 uninjured TA samples from 3 mice, Hypoxia n=12 uninjured TA samples from 12 mice. p=0.3009.

CHAPTER 4

DISCUSSION AND CONCLUSION

The effect of hypoxia on muscle atrophy have long been observed, but the molecular biology mechanisms behind this is not well understood. Since COPD and PAD patients suffer from muscle atrophy, we believe that there is a correlation between hypoxia, muscle homeostasis, and muscle regenerative capacity. Previous studies have utilized C2C12 myoblasts under hypoxic conditions to understand the signaling pathway associated with HIFs. These studies outlined the role of Hif2α and its effect on stemness of stem cells. There have also been studies that examined the role of HIFs on satellite cell proliferation and differentiation at an *in vitro* level, which are similar to the ideas that we address in this study. However, this study explored the effect of hypoxia on muscle regenerative capacity and probed the possible associated autophagic mechanisms behind muscle atrophy at an *in vivo* level. This allowed us to mimic the chronic hypoxic conditions that COPD patients endure, and to confirm on an organismal level how hypoxia affects muscle regeneration and muscle atrophy.

This study is predicated on the fact that muscle atrophy has been observed in COPD patients and other people who experience chronic hypoxia, such that it could affect muscle regenerative capacity. Ascertaining the validity of this statement and to prove whether this effect could be replicated in a laboratory setting had to be performed. We confirmed that there are significant differences between mice that were exposed to chronic hypoxia versus those that were under a normoxic environment. Following this confirmation, the knowledge that Hif2α is expressed under chronic hypoxic conditions

led us to use the conditional Hif2α KO mouse to see if deletion of this gene could rescue muscle regenerative capacity. Aside from confirming a delay in muscle regeneration, the first part of this project also aimed to validate this hypoxic effect with special hypoxia instruments in an animal mouse model. These preliminary experiments enabled us to recognize the limitations and strengths of this type of experiment. One strength of our mouse model is that we examined hypoxia as a singular common variable in patients with COPD, PAD, or live in higher altitudes above sea level. We did not strictly use a COPD or PAD animal model, since those are more complex diseases that have multiple mechanisms that cause their pathogenesis. The second strength was to be able to freely adjust the oxygen concentrations to expose the mice to varying levels of hypoxia. The obvious limitation is a small margin for error in these experiments. Slight adjustments to the mixed input gas could drastically change the amount of hypoxia within the chambers. Intramuscular cardiotoxin injections had to be consistent to induce complete damage in the TA muscle. With all experimental parameters held constant, muscle regenerative response between different mice, even littermates, could have high variability if one of these steps were inconsistent with the other experimental groups.

With our hypoxia instrument, we successfully induced a deleterious effect on muscle regenerative capacity at 14%-15% oxygen concentration with wildtype mice. Under hypoxia, the variable morphology of the regenerating myoblasts, depicted with eMyHC expression, demonstrated a delay in the regenerative profile in hypoxic mice. With the distribution curve for eMyHC+ myoblast sizes, the rightward shift in normoxic muscle showed that these myoblasts have had a longer time to regenerate and increase in size, while hypoxic eMyHC+ myoblasts were smaller by comparison. Over

the 4 dpi and 7 dpi time points, the number of proliferating (Pax7+/Ki67+) and quiescent (Pax7+/Ki67-) SCs in hypoxia remained consistently lower than normoxia. The lowered number of proliferating SCs could means that either SCs are not proliferating as quickly as normoxic muscle, or that most SCs have already proliferated and transitioned to differentiation. We see that the latter is not the case, seeing that myogenin expression was insignificantly different, so the rate of SCs transitioning to differentiating Myog+ myoblasts is unchanged. However, given the different sizes of eMyHC+ myoblasts, it can be said that the amount of maturation of these differentiating cells in terms of increase in size is delayed or defective in the hypoxic muscle. Since no further time points were taken past the 7 dpi time point in this part of the experiment, only extending the number of days to examine its muscle histology can tell us whether the differentiating myoblasts will ever increase in size, as an indication of delay.

In the following experiments dealing with the Hif2α genetic KO, we found that the Hif2α KO mouse seemed to have improved muscle regeneration. At 4 dpi, the Pax7+/Ki67+ proliferating SC count was lower than control. The Pax7+/Ki67- self-renewing SC count was also lower in the Hif2α KO TA; however, this statistic is negligible since the number of these self-renewing SCs was very low to begin with. These Hif2α SCs apparently have transitioned to the differentiation phase earlier than control, as differentiation biomakers of eMyHC cell size and Myog+ cells were higher. Later at the 9 dpi time point, the proliferating SC count justifiably decreased, since many SCs would have completed the proliferation stage after 9 dpi. Self-renewed SC count increased to higher numbers than all experimental wildtype mice in hypoxia, an indication that myogenic cell fate for most SCs have completed and the subpopulation

of proliferating SCs have returned to quiescence. Centrally nucleated myoblasts serve as an indicator for already-differentiated SCs. More mature myoblasts are bigger in size, and the distribution curve for centrally nucleated myoblasts were shifted to the right with the Hif2α KO myoblasts.

Finally, given the extra 2 days over a 7 dpi time point, it generated a more complete perspective of SC proliferation and differentiation under hypoxia. There was little deviation across 4 to 9 dpi time points in terms of the proliferating (Pax7+/Ki67+) SC count, and differentiating (Myog+) SCs counts increased by about 50%. The number of self-renewed SCs also increased dramatically at the 9 dpi time point, much like the Hif2α KO TA but to a lesser extent. This shows that muscle regeneration in hypoxia is possibly delayed starting from the SC proliferation phase, since proliferation is consistently high in the wildtype control. The wildtype control mouse at 9 dpi also had an average centrally nucleated myoblast size of 2000 pixels, where it shows the potential size that the smaller and less mature eMyHC+ cells of ~500 pixels can reach if given enough time. This means that it is more likely that there is a delay in muscle regeneration under hypoxia, rather than a size-limiting defect that would cause myoblasts to never reach normal maturation sizes.

The other specific aim addressed in this study is whether autophagy regulation has a role in muscle atrophy. We examined a small subset of our hypoxia mice to determine if the atrophied muscles expressed autophagic markers such as Atg12 and LC3A/B. The Western blot analysis demonstrated that hypoxic mice had downregulated expression of Atg12 and LC3A/B, but unfortunately atrophy could not be confirmed due to the lack of atrophy marker Atrogin-1 expression. In hindsight, the amount of hypoxia

induced at 13% to 14% oxygen concentration was probably not enough to induce enough atrophy over the 3-week experimental period. Percent body weights of the uninjured TA muscles when compared to normoxic muscle were only slightly reduced and not enough to achieve statistical significance. What is probably true is that hypoxia downregulates autophagic flux in whole muscle, but the affected phenotype remains unconfirmed. Additional studies will need to be performed in the future to confirm its role in muscle atrophy.

This research lends the possibility for Hif2α to be a therapeutic target for maintaining muscle homeostasis under hypoxic conditions. We observed the improved muscle regenerative phenotype by quantitatively measuring the SC behavior from the deletion of this gene in SCs. One possibility for the improved muscle regeneration is because Hif2α has been shown to upregulate Oct4, which in turn promotes stem cell renewal. In theory, if Hif2α is inhibited or downregulated, it would prevent Oct4 expression and prevent proliferating SCs from entering the self-renewal quiescent SC state and indirectly promote the cell towards a differentiated fate. In future experiments after this project, RNA analysis of the TA muscle could also provide insight about possibly yet unknown regulators of muscle regeneration in association with a hypoxic environment. If the theory on Hif2α holds true, it could be a way for COPD and other patients whom suffer from chronic hypoxemia to reduce the comorbid symptom of reduced muscle homeostasis and provide an extension to a higher quality of life without muscle atrophy.

REFERENCES

Barberi, L., Scicchitano, B. M., De Rossi, M., Bigot, A., Duguez, S., Wielgosik, A., . . . Musarò, A. (2013). Age-dependent alteration in muscle regeneration: the critical role of tissue niche. *Biogerontology, 14*(3), 273-292. doi:10.1007/s10522-013-9429-4

Boyer, L. A., Lee, T. I., Cole, M. F., Johnstone, S. E., Levine, S. S., Zucker, J. P., . . . Young, R. A. (2005). Core Transcriptional Regulatory Circuitry in Human Embryonic Stem Cells. *Cell, 122*(6), 947-956. doi:10.1016/j.cell.2005.08.020

Cavanagh, B. L., Walker, T., Norazit, A., & Meedeniya, A. C. (2011). Thymidine analogues for tracking DNA synthesis. *Molecules, 16*(9), 7980-7993. doi:10.3390/molecules16097980

Chaillou, T., & Lanner, J. T. (2016). Regulation of myogenesis and skeletal muscle regeneration: effects of oxygen levels on satellite cell activity. *The FASEB Journal, 30*(12), 3929-3941. doi:10.1096/fj.201600757R

Covello, K. L., Kehler, J., Yu, H., Gordan, J. D., Arsham, A. M., Hu, C.-J., . . . Keith, B. (2006). HIF-2α regulates Oct-4: effects of hypoxiaon stem cell function, embryonic development, and tumor growth. *Genes & Development, 20*(5), 557-570. doi:10.1101/gad.1399906

Dong, X., Su, X., Yu, J., Liu, J., Shi, X., Pan, Q., . . . Cao, H. (2017). Homology modeling and molecular dynamics simulation of the HIF2α degradation-related HIF2α-VHL complex. *Journal of Molecular Graphics and Modelling, 71*, 116-123. doi:http://dx.doi.org/10.1016/j.jmgm.2016.11.011

Egerman, M. A., & Glass, D. J. (2014). Signaling pathways controlling skeletal muscle mass. *Critical Reviews in Biochemistry and Molecular Biology, 49*(1), 59-68. doi:10.3109/10409238.2013.857291

Eliasson, P., Rehn, M., Hammar, P., Larsson, P., Sirenko, O., Flippin, L. A., . . . Jönsson, J.-I. (2010). Hypoxia mediates low cell-cycle activity and increases the proportion of long-term–reconstituting hematopoietic stem cells during in vitro culture. *Experimental Hematology, 38*(4), 301-310.e302. doi:http://dx.doi.org/10.1016/j.exphem.2010.01.005

Fu, X., Wang, H., & Hu, P. (2015). Stem cell activation in skeletal muscle regeneration. *Cellular and Molecular Life Sciences, 72*(9), 1663-1677. doi:10.1007/s00018-014-1819-5

García-Prat, L., Martínez-Vicente, M., Perdiguero, E., Ortet, L., Rodríguez-Ubreva, J., Rebollo, E., . . . Muñoz-Cánoves, P. (2016). Autophagy maintains stemness by preventing senescence. *Nature, 529*(7584), 37-42. doi:10.1038/nature16187

http://www.nature.com/nature/journal/v529/n7584/abs/nature16187.html#supplementary-information

Gosker, H. R., Engelen, M. P., van Mameren, H., van Dijk, P. J., van der Vusse, G. J., Wouters, E. F., & Schols, A. M. (2002). Muscle fiber type IIX atrophy is involved in the loss of fat-free mass in chronic obstructive pulmonary disease. *The American Journal of Clinical Nutrition, 76*(1), 113-119.

Gruber, M., Hu, C.-J., Johnson, R. S., Brown, E. J., Keith, B., & Simon, M. C. (2007). Acute postnatal ablation of Hif-2α results in anemia. *Proceedings of the National Academy of Sciences of the United States of America, 104*(7), 2301-2306. doi:10.1073/pnas.0608382104

Karalaki, M., Fili, S., Philippou, A., & Koutsilieris, M. (2009). Muscle regeneration: cellular and molecular events. *In Vivo, 23*(5), 779-796.

Keith, B., Johnson, R. S., & Simon, M. C. (2011). HIF1α and HIF2α: sibling rivalry in hypoxic tumor growth and progression. *Nature reviews. Cancer, 12*(1), 9-22. doi:10.1038/nrc3183

Kim, J.-w., Tchernyshyov, I., Semenza, G. L., & Dang, C. V. (2006). HIF-1-mediated expression of pyruvate dehydrogenase kinase: A metabolic switch required for cellular adaptation to hypoxia. *Cell Metabolism, 3*(3), 177-185. doi:http://dx.doi.org/10.1016/j.cmet.2006.02.002

Krock, B. L., Skuli, N., & Simon, M. C. (2011). Hypoxia-Induced Angiogenesis: Good and Evil. *Genes & Cancer, 2*(12), 1117-1133. doi:10.1177/1947601911423654

Kuang, S., Gillespie, M. A., & Rudnicki, M. A. (2008). Niche Regulation of Muscle Satellite Cell Self-Renewal and Differentiation. *Cell Stem Cell, 2*(1), 22-31. doi:http://dx.doi.org/10.1016/j.stem.2007.12.012

Lang, K. C., Lin, I. H., Teng, H. F., Huang, Y. C., Li, C. L., Tang, K. T., & Chen, S. L. (2009). Simultaneous overexpression of Oct4 and Nanog abrogates terminal myogenesis. *American Journal of Physiology - Cell Physiology, 297*(1), C43-C54. doi:10.1152/ajpcell.00468.2008

Liao, D., Corle, C., Seagroves, T. N., & Johnson, R. S. (2007). Hypoxia-Inducible Factor-1α Is a Key Regulator of Metastasis in a Transgenic Model of Cancer Initiation and Progression. *Cancer Research, 67*(2), 563-572. doi:10.1158/0008-5472.can-06-2701

Liu, Z.-j., Semenza, G. L., & Zhang, H.-f. (2015). Hypoxia-inducible factor 1 and breast cancer metastasis. *Journal of Zhejiang University. Science. B, 16*(1), 32-43. doi:10.1631/jzus.B1400221

Lőw, P., Varga, Á., Pircs, K., Nagy, P., Szatmári, Z., Sass, M., & Juhász, G. (2013). Impaired proteasomal degradation enhances autophagy via hypoxia signaling in Drosophila. *BMC Cell Biology, 14*(1), 29. doi:10.1186/1471-2121-14-29

Mann, C. J., Perdiguero, E., Kharraz, Y., Aguilar, S., Pessina, P., Serrano, A. L., & Muñoz-Cánoves, P. (2011). Aberrant repair and fibrosis development in skeletal muscle. *Skeletal Muscle, 1*(1), 21. doi:10.1186/2044-5040-1-21

Mauro, A. (1961). SATELLITE CELL OF SKELETAL MUSCLE FIBERS. *The Journal of Biophysical and Biochemical Cytology, 9*(2), 493-495.

Maxwell, P. H., Wiesener, M. S., Chang, G.-W., Clifford, S. C., Vaux, E. C., Cockman, M. E., . . . Ratcliffe, P. J. (1999). The tumour suppressor protein VHL targets hypoxia-inducible factors for oxygen-dependent proteolysis. *Nature, 399*(6733), 271-275. doi:http://www.nature.com/nature/journal/v399/n6733/suppinfo/399271a0_S1.html

Murphy, M. M., Lawson, J. A., Mathew, S. J., Hutcheson, D. A., & Kardon, G. (2011). Satellite cells, connective tissue fibroblasts and their interactions are crucial for muscle regeneration. *Development (Cambridge, England), 138*(17), 3625-3637. doi:10.1242/dev.064162

Pallafacchina, G., Blaauw, B., & Schiaffino, S. (2013). Role of satellite cells in muscle growth and maintenance of muscle mass. *Nutrition, Metabolism and Cardiovascular Diseases, 23, Supplement 1*, S12-S18. doi:http://dx.doi.org/10.1016/j.numecd.2012.02.002

Passey, S. L., Hansen, M. J., Bozinovski, S., McDonald, C. F., Holland, A. E., & Vlahos, R. (2016). Emerging therapies for the treatment of skeletal muscle wasting in chronic obstructive pulmonary disease. *Pharmacology & Therapeutics, 166*, 56-70. doi:http://dx.doi.org/10.1016/j.pharmthera.2016.06.013

Sandri, M. (2010). Autophagy in skeletal muscle. *FEBS Lett, 584*. doi:10.1016/j.febslet.2010.01.056

Semenza, G. L. (2011). Regulation of Metabolism by Hypoxia-Inducible Factor 1. *Cold Spring Harbor Symposia on Quantitative Biology, 76*, 347-353. doi:10.1101/sqb.2011.76.010678

Semenza, G. L. (2016a). Dynamic regulation of stem cell specification and maintenance by hypoxia-inducible factors. *Molecular Aspects of Medicine, 47–48*, 15-23. doi:http://dx.doi.org/10.1016/j.mam.2015.09.004

Semenza, G. L. (2016b). The hypoxic tumor microenvironment: A driving force for breast cancer progression. *Biochimica et Biophysica Acta (BBA) - Molecular Cell Research, 1863*(3), 382-391. doi:http://dx.doi.org/10.1016/j.bbamcr.2015.05.036

Takahashi, K., & Yamanaka, S. (2006). Induction of Pluripotent Stem Cells from Mouse Embryonic and Adult Fibroblast Cultures by Defined Factors. *Cell, 126*(4), 663-676. doi:http://dx.doi.org/10.1016/j.cell.2006.07.024

Tazuke, S. I., Mazure, N. M., Sugawara, J., Carland, G., Faessen, G. H., Suen, L.-F., . . . Giudice, L. C. (1998). Hypoxia stimulates insulin-like growth factor binding protein 1 (IGFBP-1) gene expression in HepG2 cells: A possible model for IGFBP-1 expression in fetal hypoxia. *Proceedings of the National Academy of Sciences of the United States of America, 95*(17), 10188-10193.

Tidball, J. G. (2005). Inflammatory processes in muscle injury and repair. *American Journal of Physiology - Regulatory, Integrative and Comparative Physiology, 288*(2), R345-R353. doi:10.1152/ajpregu.00454.2004

Wang, B., Wood, I. S., & Trayhurn, P. (2008). Hypoxia induces leptin gene expression and secretion in human preadipocytes: differential effects of hypoxia on adipokine expression by preadipocytes. *Journal of Endocrinology, 198*(1), 127-134. doi:10.1677/joe-08-0156

Wüst, R. C. I., & Degens, H. (2007). Factors contributing to muscle wasting and dysfunction in COPD patients. *International Journal of Chronic Obstructive Pulmonary Disease, 2*(3), 289-300.

Yang, X., Yang, S., Wang, C., & Kuang, S. (2017). The hypoxia-inducible factors HIF1alpha and HIF2alpha are dispensable for embryonic muscle development but essential for postnatal muscle regeneration. *J Biol Chem, 292*(14), 5981-5991. doi:10.1074/jbc.M116.756312

Yuan, L., Han, J., Meng, Q., Xi, Q., Zhuang, Q., Jiang, Y., . . . Wu, G. (2015). Muscle-specific E3 ubiquitin ligases are involved in muscle atrophy of cancer cachexia: an in vitro and in vivo study. *Oncol Rep, 33*(5), 2261-2268. doi:10.3892/or.2015.3845

Zhao, J., Brault, J. J., Schild, A., Cao, P., Sandri, M., Schiaffino, S., . . . Goldberg, A. L. (2007). FoxO3 Coordinately Activates Protein Degradation by the Autophagic/Lysosomal and Proteasomal Pathways in Atrophying Muscle Cells. *Cell Metabolism, 6*(6), 472-483. doi:http://dx.doi.org/10.1016/j.cmet.2007.11.004

APPENDIX

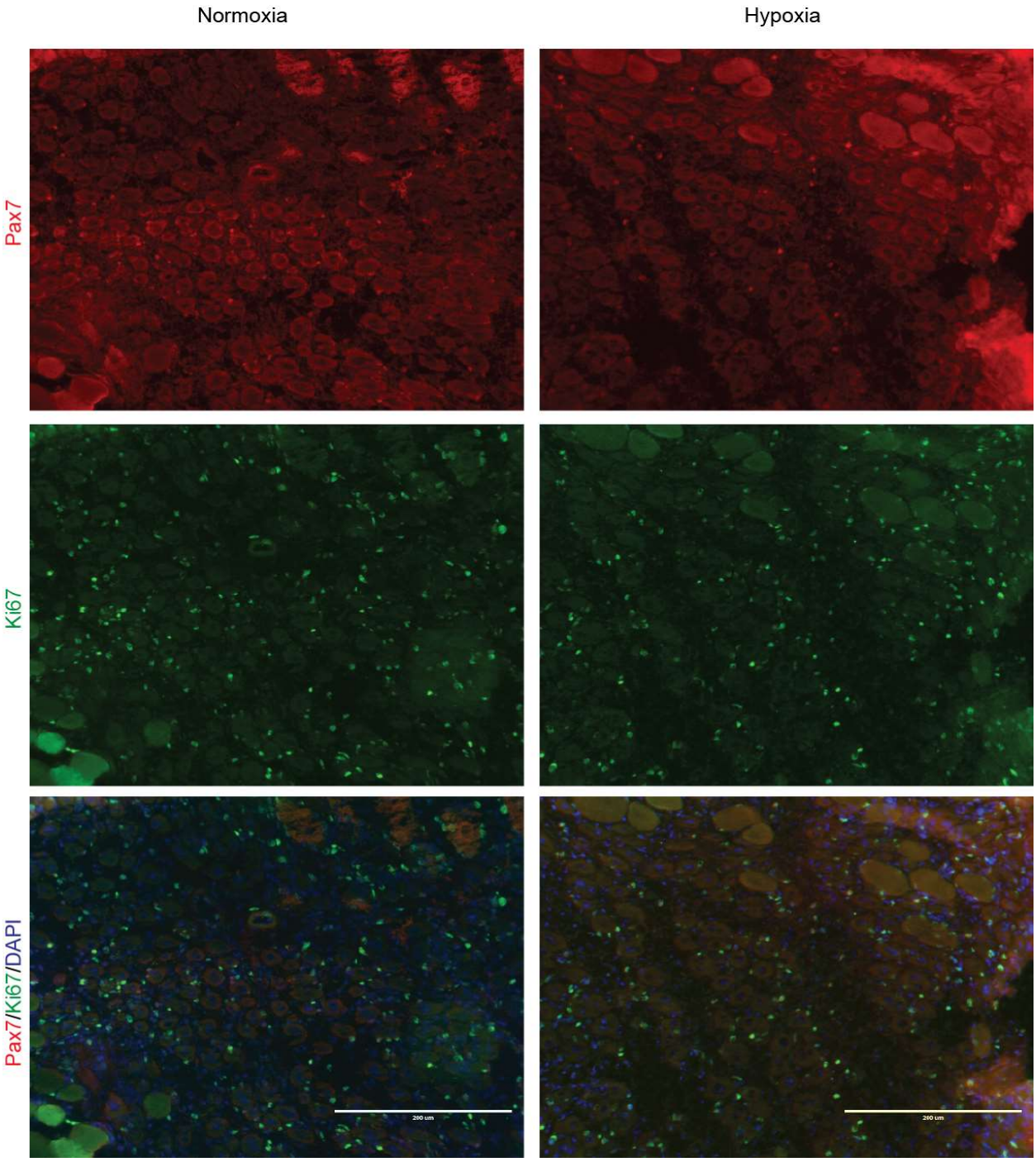

Appendix A **Pax7/Ki67 colocalization at 4 dpi WT TA muscle under normoxia/hypoxia.**

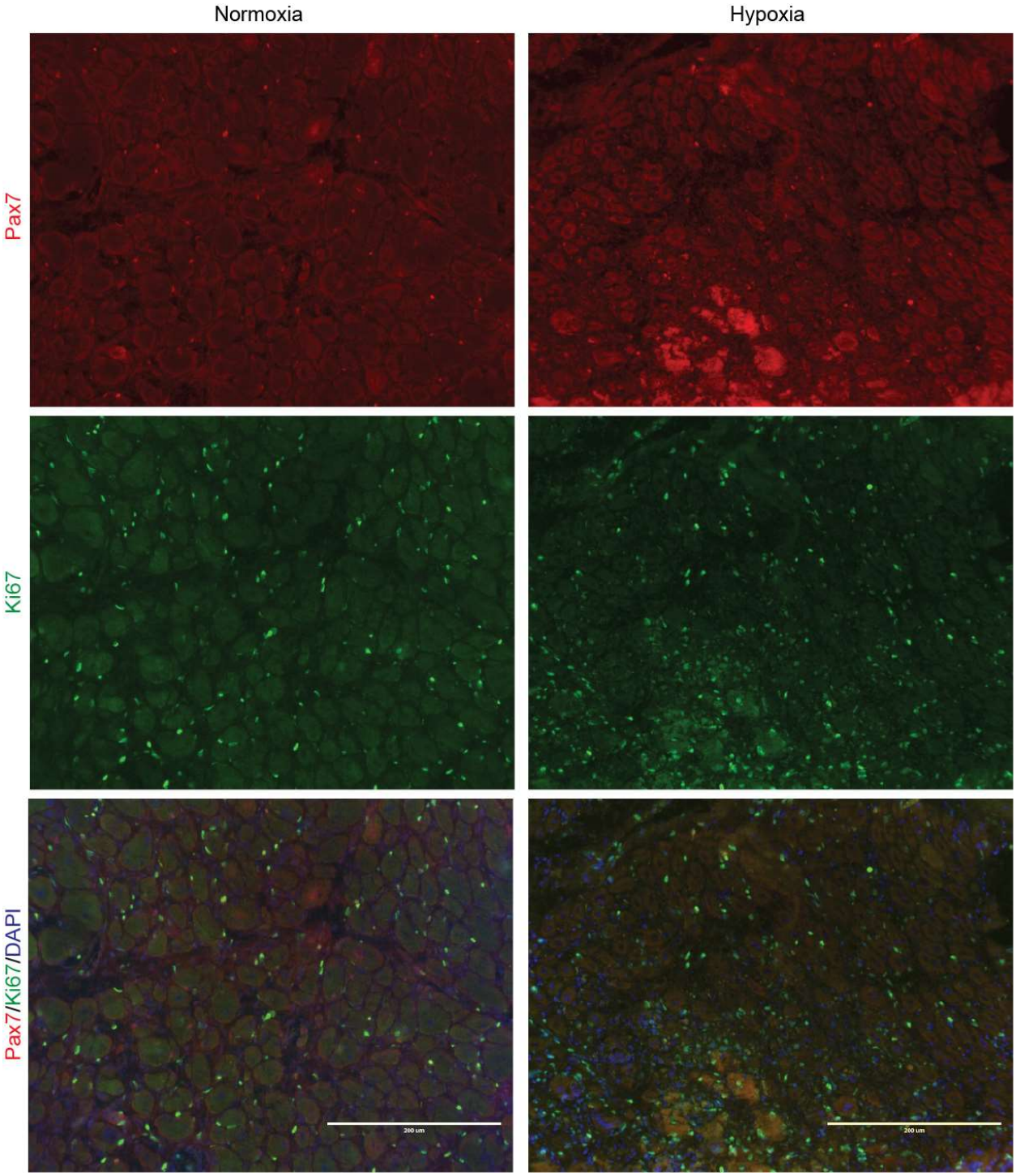

Appendix B **Pax7/Ki67 colocalization at 7 dpi WT TA muscle under normoxia/hypoxia.**

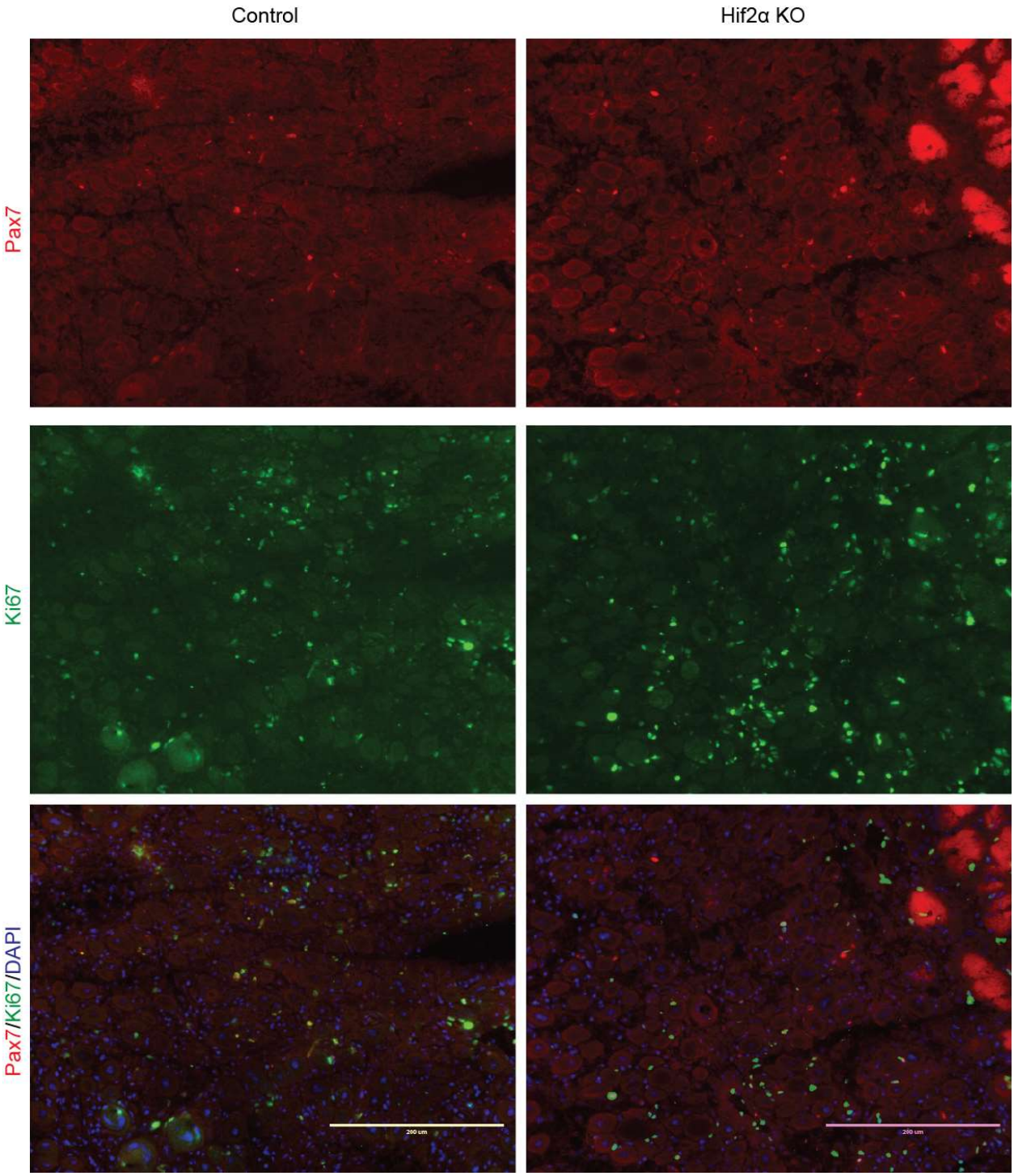

Appendix C **Pax7/Ki67 colocalization at 4 dpi Hif2α KO TA muscle under hypoxia.**

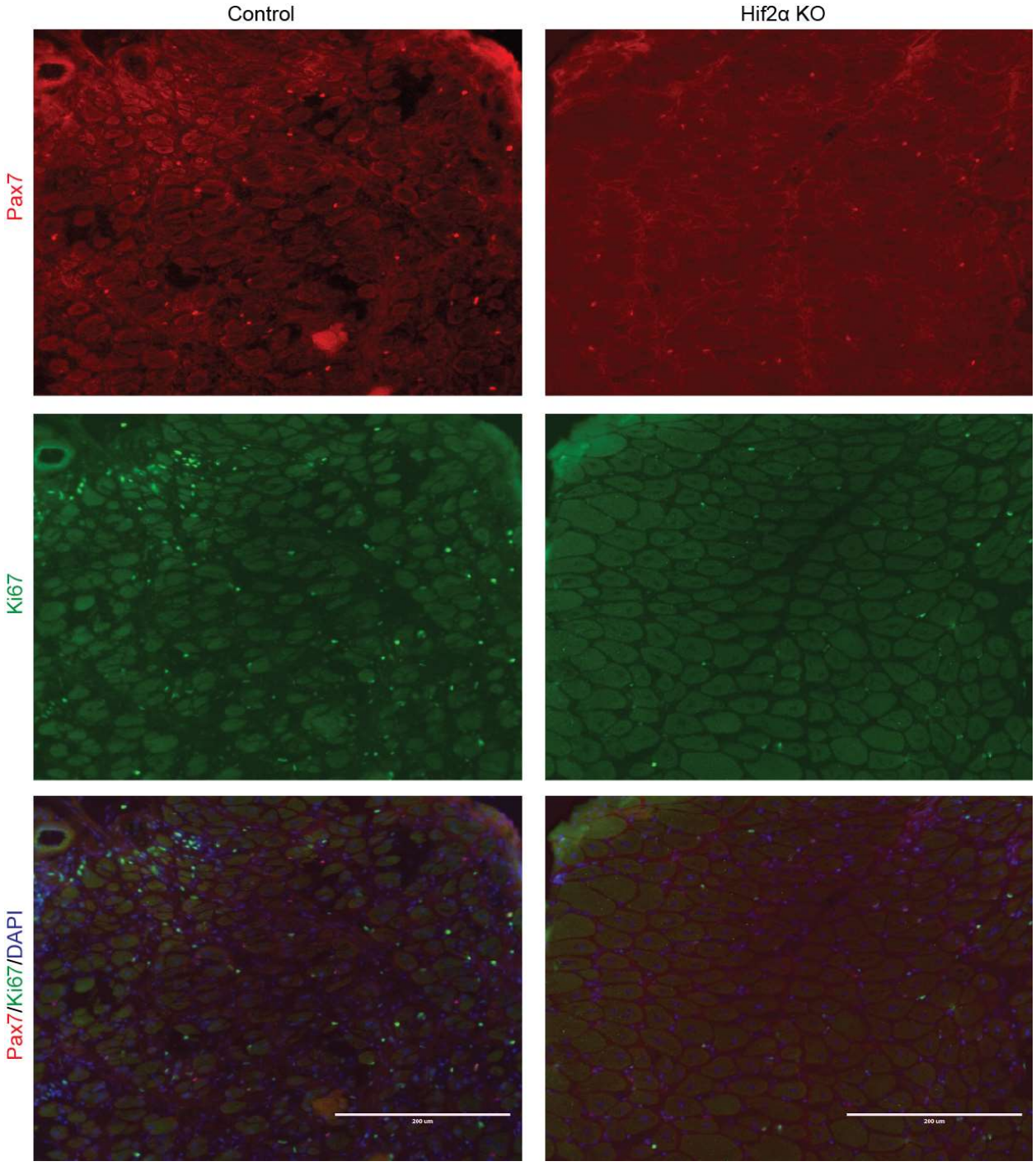

Appendix D **Pax7/Ki67 colocalization at 9 dpi Hif2α KO TA muscle under hypoxia.**